**Paper Number:**
DOE/MC/30176-97/C0823

**Title:**
Three Dimensional Characterization and Archiving System

**Authors:**
R. Clark
P. Gallman
J. Gaudreault
R. Mosehauer
A. Slotwinski
G. Jarvis
P. Griffiths

**Contractor:**
Coleman Research Corporation
6551 Loisdale Court, Suite 800
Springfield, VA 22150

**Contract Number:**
DE-AC31-93MC30176

**Conference:**
Industry Partnerships to Deploy Environmental Technology

**Conference Location:**
Morgantown, West Virginia

**Conference Dates:**
October 22-24, 1996

**Conference Sponsor:**
Morgantown Energy Technology Center

# Disclaimer

# Three Dimensional Characterization and Archiving System

Robert Clark (bob_clark@mail.crc.com); 703-719-9200)
Philip Gallman (phil_gallman@mail.crc.com); 703-719-9200)
James Gaudreault (jim_gaudreault@mail.crc.com); 703-719-9200)
Richard Mosehauer (richard_mosehauer@mail.crc.com); 703-719-9200)
Anthony Slotwinski (tony_slotwinski@mail.crc.com); 703-719-9200)
Coleman Research Corporation
6551 Loisdale Court, Suite 800
Springfield, VA 22150

George Jarvis (617-938-0651)
Thermedics Detection, Inc.
220 Mill Road
Chelmsford, MA 01824

Peter Griffiths (208-885-7814)
Department of Chemistry
University of Idaho
Moscow, ID 83844

## 1.0 Introduction

The Three Dimensional Characterization and Archiving System (3D-ICAS)[1] is being developed as a remote system to perform rapid in situ analysis of hazardous organics and radionuclide contamination on structural materials. Coleman Research and its subcontractors, Thermedics Detection, Inc. (TDI) and the University of Idaho (UI) are in the final phase of a three phase program to develop 3D-ICAS to support Decontamination and Decommissioning (D&D) operations. Accurate physical characterization of surfaces and radioactive and organic contamination is a critical D&D task. Surface characterization includes identification of potentially dangerous inorganic materials, such as asbestos and transite.

Real-time remotely operable characterization instrumentation will significantly advance analysis capabilities beyond those currently employed. Chemical analysis is a primary area where the characterization process will be improved. Chemical analysis plays a vital role throughout the process of decontamination. Before clean-up operations can begin the site must be characterized with respect to the type and concentration of contaminants, and detailed site mapping must clarify areas of both high and low risk. During remediation activities chemical analysis provides a means to measure progress and to adjust clean-up strategy. Once the clean-up process has been completed the results of chemical analysis will verify that the site is in compliance with federal and local regulations.

[1]Research sponsored by the U.S. Department of Energy's Morgantown Technology Center, under contract DE-AC31-93MC30176 with Coleman Research Corporation, 6551 Loisdale Court, Springfield, VA 22150; fax 703-719-9229.

The development of the field operable in situ analysis capability of the 3D-ICAS will result in a significantly improved capability to perform analyses for trace organic compounds and radionuclides by providing real-time quantitative results on-site. This will greatly improve the effectiveness of Department of Energy (DOE) response to identified sites by streamlining the entire beginning-to-end process from the initial contamination surveys, through monitoring the progress of site restoration efforts, and determining when regulatory standards have been met. The field operable remotely directed analysis instrumentation of 3D-ICAS will have great impact in terms of:

- Improving the quality and efficiency of site clean-up activities
- Reducing health and safety risks to the survey workers
- Reducing the associated cost and time required for remediation
- Reducing waste generation

## 2.0 The Approach

The 3D-ICAS system robotically conveys a multisensor probe near the surfaces to be inspected. The sensor position and orientation are monitored and controlled using coherent laser radar (CLR) tracking. The CLR also provides 3D facility maps which establish a 3D “world view” within which the robotic sensor system can operate.

The 3D-ICAS fills the need for high speed automated organic analysis by means of a gas chromatographs-mass spectrometer (GC/MS) sensor which can process a sample, without direct contact, accomplishing detection and fine grain analysis of regulatory concentrations (EPA 1987 spill cleanup policy: 1µg/10cm$^2$ for high use interior building surfaces) in approximately one minute. This compares with traditional GC/MS laboratory analysis methods which involves sample preparation and waste generation, and take hours per sample for analysis. The 3D-ICAS GC/MS sensor extracts volatile organics directly from contaminated surfaces without sample removal, then uses multiple stage focusing to accomplish high time resolution insertion into a high speed gas chromatograph. Detection and additional discrimination are provided by a final stage time-of-flight mass spectrometer (TOF-MS). This high speed process replaces sample collection and transport and hours of solution preparation before injection into an ordinary GC/MS which typically has a 45 minute run time.

The radionuclide sensors of the 3D-ICAS multisensor probe combines $\alpha$, ß, and $\gamma$ counting with energy discrimination on the $\alpha$ channel. This sensor combination identifies and quantifies isotopes of specific DOE interest of uranium, plutonium, thorium, technetium, neptunium, and americium to regulatory levels in approximately one minute.

The Molecular Vibrational Spectrometry (MVS) sensor of the multisensor probe is used to characterize substrate material such as concrete, transite, wood or asbestos. The surface composition information provided by the MVS can be used to provide estimates of the depth of contamination and to optimize the analysis performance of the other contamination detection sensors. In addition, the materials composition information, combined with the surface geometry maps provided by the coherent laser radar, will provide a more complete three dimensional world view to be used to plan and execute robotic D&D operations.

The 3D-ICAS will scan operator designated areas with a full sensor set or a selected subset at a designated sample density. The 3D-ICAS will plan and monitor the sensor trajectory to assure efficient, close sensing without surface contact.

The 3D-ICAS sensor output and contamination analysis along with CLR position information will be available for real-time monitoring immediately after each one to two minute sample period. After a surface mapping operation is completed, 3D-ICAS will provide three dimensional displays showing contours of detected contaminant concentrations. The 3D-ICAS will further provide permanent measurement data and contaminant level archiving, assuring data integrity and allowing straightforward regulatory review of the characterization process before and after D&D operations.

Figure 2-1 shows the interconnection of the major subsystems. The links are a combination of serial for slow speed command and control, TCP/IP network for file based data file storage and communications, and dedicated analog and digital links for high bandwidth functions such as servo loops, gas chromography, and laser radar transmission and reception.

The Integrated Workstation (IWOS) communications with the TCP/IP network based link to the CLR control computer. This link provides all hardware control functions and database access for the Integrated Workstation.

The CLR computer serves as a focal point for hardware control. Serial links are used between the CLR computer and the Multisensor Probe (MSP) electronics control computer to provide control and status information. Data from the Multisensor Probe is stored directly on a TCP/IP network drive. Serial links are also used to control the robot arm position. The 3D-ICAS Phase II demonstration multisensor probe is shown in Figure 2-2.

Not shown in Figure 2-1 are the remotely operated platforms providing independent mobility for the robot arm and the CLR mapper/tracker. The robot arm platform is used to move the arm anywhere in the volume to be surveyed while the robot arm itself provides precise positioning and orientation for the multisensor probe. The CLR mapper platform is used during both mapping and survey operations to provide optimum perspectives. The data link between the mapper and CLR electronics will be via RF, permitting tetherless operation.

## 3.0 The Development Program

The 3D-ICAS is being developed in a three phase program. Phase I demonstrated the GC/MS sensor system breadboard. Phase II provided integration of the GC and MS subsystems,

integration of the multisensor probe with the robot arm and the coherent laser radar tracker. The Phase II 3D-ICAS demonstration, involving contamination surface mapping with a CLR guided, robotically maneuvered multisensor probe, occurred in November, 1995.

The Phase III system will integrate and test the total system in a mobile field prototype and demonstrate the systems at ORNL in mid to late 1997.

A substantial part of the development effort is the integration of the 3D CLR mapping and robotic sensor positioning and tracking capability with the sensor data output in a common coordinate frame so that 3D archiving of contamination surveys can take place. This paper will not discuss detailed system integration issues, but will discuss areas of developing technical performance of the GC/MS sensor, the radionuclide sensor, the MVS sensor, and the CLR 3D mapper and six degrees of freedom (6-DOF) end effector tracker which are of interest to the 3D-ICAS user.

### 3.1 High Speed Gas Chromatograph/Mass Spectrometer Subsystem

The current effort consisted of employing state of the art components and developing additional components and software such that definitive quantitative measurement of organic contamination on building surfaces could be made in less than one minute. A block diagram of the major modules and interconnections of the High Speed Gas Chromatograph/Mass Spectrometer (HSGC/MS) Sensor is shown in Figure 3-1.

#### 3.1.1 Mass Spectrometer

This effort required review of mass spectrometer requirements for utilization as a detector for the high speed gas chromatograph, review concepts for integration to HSGC, review pertinent literature and vendor documentation and based on this knowledge base procure a mass spectrometer.

A time-of-flight mass analyzer system (TOF-MS) was chosen based on its ability to maintain a high data throughput. Early on it was determined that effective High Speed GC/MS would require a detector system capable of complete mass scans in 15 millisecond or less. The time-of-flight system is the only mass analyzer capable of such a scanning rate.

The TOF-MS is an operationally simple and reliable form of mass spectrometer. All mass spectrometers have some form of interface to the outside world, all require high vacuum chambers, all require ionization sources and all require detectors. In general what differentiates mass spectrometers is the technology for mass analysis. For 3D-ICAS, a very fast detector is require to fully utilize the capabilities of the high speed GC technology and hence be compatible with near real time definitive detection. A time-of-flight mass analyzer was chosen because it can provide full mass spectral scan (to 600 amu) for every ionization event. Other types of mass spectrometers cannot generate full mass spectra at these high rates. The full mass spectra is necessary for identification of the unknown components of a sample through library searching. Finally, existing TOF technology will allow high repetition scan rates for implementing high duty cycle, high speed operation of the TOF-MS detector when coupled to the High Speed GC.

The TOF-MS generates a complete mass spectrum across the mass range 35 to 600 amu every 100 microseconds. 128 mass scans are added together to give an integrated mass spectrum corresponding to 12.8 milliseconds of GC elution time. This integration process yields a signal-to-noise improvement of approximately 11. The ion intensities of the integrated mass spectrum are then summed to generate the total ion chromatogram.

The high data rate of the TOF-MS can be utilized for GC peak deconvolution. Every 12.8 milliseconds a high quality, full scan mass spectrum is measured. Since the mass spectra are high quality, full scan, the data from neighboring GC times can be compared for GC peak deconvolution. For example, a GC peak that has a 500 milliseconds base width will have 32 full scan mass recorded across the peak. A matching comparison of the successive mass spectra will indicate if analytes are coeluting. Algorithms have been developed which compare mass spectra across a GC peak for deconvolution of coeluting analytes. Other mass analysis technologies cannot provide mass spectra at data rate high enough to be useful detector for high speed GC. Additionally the high data rates of the TOF-MS are exploited in GC peak deconvolution algorithms providing further additional improvements in data quality.

In Phase III, the TOF-MS is being miniaturized for substantial reduction in both size and weight. The MS electronics are being redesigned for simple computer operation that is specific to this application. Initial performance testing indicates a resolution sufficient for organic compound identification.

One of the most critical parts of a GC/MS is the interface between the systems. The interface plays the important role in both accommodating the pressure drop from the GC column to the MS ionization source and enriching the concentration of analyte in the carrier gas after passing through the interface into the mass spectrometer. In general the pressure drop is accommodated by removing as much of the carrier gas as possible. A variety of technologies are available for the removing carrier gas in a GC/MS interface. Briefly, the requirements for a GC/MS interface are high transfer efficiency, no impact on the GC separation, no degradation of compounds, no preferential removal of compounds or chemical functional groups. In addition to these requirements the interface in this effort must operate on a fast time scale. Of all the techniques available the concept of a molecular beam interface was chosen as optimal.

A molecular beam GC to MS interface consists of a heated transfer line to efficiently carry the GC column effluent into a vacuum expansion chamber. The GC column is held in an XYZ translation stage for alignment with a skimmer nozzle. The GC column and skimmer are held in close proximity. As the GC column effluent exits the column the lighter carrier gas either helium or hydrogen diffuses away from the sample analytes in the vacuum region. The heavier sample analytes are transferred through the skimmer nozzle in a directed beam with the momentum of the carrier gas. In this approach the carrier gas is removed and the analytes are enriched into a directed beam of molecules. The directed beam of molecules is aligned with the XYZ translator through the skimmer to intersect the electron gun beam in the ionization source. The introduction of the molecules into the ionization source of the MS in this manner removes the carrier gas, enriches the analyte and generates a directed beam of molecules into the electron gun beam for ionization.

The directed beam of molecules has an advantage over conventional thermal, diffusive methods for introduction of the molecules into the ionization source. The concentration of molecules within the volume of space that the electron gun molecular beam cross is enhanced. With the enhanced concentration of molecules in the electron gun beam the probability of ionization per unit time is increased thereby increasing sensitivity.

In Phase III, the GC to MS interface has been miniaturized and simplified. The XYZ stage has been eliminated and a simple fixed design has been implemented. The external mechanical pump has been eliminated. The region is pumped using the upper stage of a dual stage turbo molecular pump. The features of the molecular beam interface remain with a less complex more ruggardized version of the hardware.

### 3.1.2 GC/MS Processing

A block diagram of the sensor data acquisition and processing system interconnection is shown in Figure 3-2. The overall function of these components are to acquire the time-of-flight MS data as a function of GC elution time, control the GC operation, control the radionuclide detectors for data collection and processing. The details on the radionuclide detectors are in section 3.2. The acquired data from the GC/MS sensor is processed into mass spectra and a total ion chromatogram. The GC/MS data are processed through a National Institutes of Standards and Technology (NIST) Mass Spectral Database, response factor calibration and sample classification algorithms for further data reduction. The acquired data from the Radionuclide sensor is processed into both an alpha spectrum and a beta/gamma level. The alpha spectrum is discriminated into activity levels for different isotopes, U-235, U-238, Am-241, Pu-239, Pu-242 and Th-230 and the beta/gamma level is reported as activity of Tc-99. The electronics technology contains high speed state of the art components which are compatible with the operation of the sensor hardware.

The electronics technology for the HSGC-MS data acquisition and processing are a high speed transient digitizer, a high speed data transfer bus at 20 Mb/sec and a high speed digital signal processor. Since the TOF-MS events occur on a nanosecond time-scale, the transient digitizer is used to accurately determine the data burst. Mass spectral scale from 35 to 600 amu requires approximately 40 microseconds of data with the individual MS peaks being approximately 15 to 30 nanoseconds wide at the half height. Thus, to achieve mass spectral resolution of 1 amu at 600 amu 5 to 10 nanosecond time discrimination is required. The transient digitizer is capable of summing the data burst waveforms in onboard memory to allow signal averaging. At this point in the data flow the full mass spectrum is represented as time data with a resolution of 5 nanoseconds. The data records are transferred from the transient digitizer to the digital signal processor over a high speed data transfer bus at 20 Mb/second. This high speed transfer is used to recycle the transient digitizer for the next set of data. The high speed digital signal processor performs many crucial functions in the initial stages of the data processing. These function include the conversion of the time-of-flight data into mass spectral scale data, detects the occurrence of the GC peaks and determine if the detected GC peak is comprised of one or two compounds, e.g., identifies coeluting compounds. Once the GC and MS information are extracted from the raw data on the high speed digital signal processor, the data are transferred to the overall system controller.

The high speed controller, pentium 120 MHz, performs the overall control of the multisensor subsystem including the following: initiation of the sample extraction and GC separation, timing for the transient digitizer and digital signal processor, NIST mass spectral database searching, high level data processing and summary output of the GC/MS and radionuclide sensors, and both control and data processing for the radionuclide sensor.

In Phase III, the concept for the GC/MS data acquisition and processing has not changed. The hardware has been redesigned and modified for the shorter MS flight tube. Additional improvements are expected in the areas of synchronization of the transient digitizer and ion source for improved resolution and relative peak height information.

### 3.1.3 GC/MS Test Results

The tests were carried out using the breadboard GC/MS to optimize the performance characteristics and demonstrate overall function. The function included sampling from surface, GC separation and MS detection, identification and quantification.

A successful laboratory demonstration of the integrated breadboard components of the 3D-ICAS was held in November 1995 at CRC's facility in Springfield Va. The GC/MS sensor, integrated with the Robot Controller, detected PCBs at the regulatory level[1,2] at nearly twice the expected speed of operation.

The Phase II success criterion for the GC/MS sensor is detection of organic chemicals from concrete surfaces at the regulatory level in one minute. The GC/MS sensor met this criterion by extracting, identifying and quantifying PCBs at a level of 4 μg/10 $cm^2$ on concrete with an average signal-to-noise ratio of 10 in a 40 second measurement time. This data indicates the sensitivity is 1 μg/10 $cm^2$ at nearly twice the expected speed of operation. At the Phase II demonstration, the GC/MS sensor was a functioning breadboard system capable of analyzing hydrocarbons embedded in concrete to the regulatory limit in less than one minute. This demonstrates that the GC/MS sensor exceeds the Phase II success criteria of detecting, identifying and quantifying hazardous organic chemicals from building surfaces.

A total ion chromatogram from a 4 μg/10 $cm^2$ PCB sample as measured using the integrated 3D-ICAS system is shown in Figure 3-3. To prepare the sample 20 microliters (μl) of a 0.2 μg/μl liquid standard mixture of Arochlors 1221, 1242 and 1254 (Supelco P/N48862) were placed onto the concrete block to cover an area of 10 $cm^2$. The solvent was allowed to dry for at least 30 minutes and then the measurement was initiated through the 3D-ICAS Robot Controller.

The mass spectrum of the chromatographic peak at 12.72 seconds is shown in Figure 3-4. The detailed result of the measurement, shown in Figure 3-5a, indicates that the peak at 12.72 seconds is chlorobiphenyl, a component of PCBs. The sum of all the peaks identified as PCBs or chlorinated biphenyls is 3.6 μg. The measurement area of the GC/MS sensor is 10 $cm^2$. The average signal to noise ratio across the chromatogram is 10. The detection sensitivity at a signal to noise ratio of 3 is 1.0 μg/10 $cm^2$ for a 40 second measurement and data processing time.

The GC/MS sensor data processing generates a list of chemical components which constitute the sample. As part of the data processing task, algorithms were developed to assign these chemicals into chemical classes for categorizing the sample. Shown is Figure 3-5b is the chemical classification of the results of the measurement and data processing for the sample described in Figures 3-3 to 3-5. The sample has been classified as PCBs based on the NIST database search of the mass spectra generated by the GC/MS and summing the quantities of the chemical components. Although good success has been achieved it is expected as Phase III progresses the Classification algorithm will be refined. This classification of the sample into chemical classes is used in the Integrated Work and Operating Station (IWOS) for contamination mapping. The detailed data, i.e., chromatogram, mass spectra, etc., are also available through

interrogation of the IWOS database. Operationally, a skilled chemist is expected to review the results of this classification as part of the quality assurance procedures.

To verify the High Speed GC/MS sensor generates data that are comparable to standard laboratory data a series of test were performed to examine the characteristics of the chromatograms and mass spectra. In a series of experiments the chromatograms and mass spectra for a thermally desorb samples was compared to that for syringe injections. Shown in Figure 3-6 is the chromatograms of a mixture of PCBs analyzed using syringe injection and thermal desorption. Comparison of the data indicate similar chromatographic characteristics of retention times and peak widths. The data shown in Figures 3-7, 3-8 and 3-9 are the mass spectra for chlorobiphenyl from the thermal extraction, syringe injection and NIST mass spectral database, respectively. Comparisons between these data indicate a good match to the NIST mass spectrum. This data indicates that the high speed GC/MS sensor is effective in obtaining a representative sample from surfaces such as concrete and processing the sample to produce data comparable to conventional GC/MS systems.

The GC/MS sensor was calibrated using volumes of trace level standards in solution obtained from various manufacturers. The following was the procedure used for quantitative calibration. A known volume of the standard was applied to the concrete block to cover an area of 10 $cm^2$. The solution was allowed to dry for a minimum of 30 minutes. The Multisensor probe was positioned by hand at the point to be sampled. The sampling and analysis sequence was run and the data correlated with amount of standard applied. To match the sensor spot size, 10 $cm^2$, of the High Speed GC/MS sensor, the 10 μg/100 $cm^2$ regulatory level has been expressed to 1 μg/ 10 $cm^2$.

Shown in Figure 3-10 is a calibration curve for a mixture of PCBs applied to a concrete block. The data shown good linearity, r=0.95+, over 2 orders of magnitude in response. The limit of detection was determined to be 1.0 μg/10 $cm^2$ with a signal to noise of 3. The sensing time was 40 seconds and the standoff distance was 4 mm. This data indicates that the HSGC/MS sensor has sufficient sensitivity and speed of operation for detection of PCBs at the regulatory level.

### 3.1.4 GC/MS Summary

The Phase II objective was to develop the necessary hardware and procedures for high speed GC/MS analysis of the toxic organics, using analog compounds similar to PCBs. The goal was GC separation and mass spectrometer identification in one minute to regulatory limits. The high speed GC-MS sensor is expected to accomplish GC separation, MS identification, MS library database search for identification and quantitation in less than 60 seconds. This capability will satisfy the Phase II success criteria of sampling analysis and data processing for GC/MS. Coupled with the Multisensor probe for automated sample extraction, preconcentration and transport this subsystem has established a new benchmark for speed and performance in organic analysis.

## 3.2 Radionuclide Sensors

In Phase II, effort was required for developing the overall radioisotope algorithm, testing the RN hardware, and breadboarding the components of the multisensor probe. For the radioisotopes of interest twodetectors were determined to best meet the functional needs. This was because the majority of the isotopes are alpha emitters (Am, Th, Pu, U) and one is a beta emitter (Tc). The radionuclide sensor system includes both a diffused junction silicon detector for alpha emitting isotopes and a sealed gas proportional detector for beta/gamma emitting isotopes. A multichannel analyzer is integrated with the diffused junction detector for discrimination of the alpha isotopes. This design ensures that all the isotopes of interest will be identified.

The specific alpha emitting isotopes U-238, U-235, Pu-239, Pu-242, Am-241 and Th-230 are identified and quantified. The total beta/gamma activity will be reported as Tc-99. Isotopic discrimination of beta emitters is not integrated in the current design because the current state of the art instrumentation for beta discrimination would make the MSP weight and size unmanageable. Although not done in Phase II, the gamma activity can be discriminated from the beta activity by simple mechanical shuttling of metal plate discriminators.

In the development effort for the radionuclide sensors, two systems were constructed: one for TDI to incorporate into MSP hardware and a second to remain at Eberline where appropriate facilities are available for testing and optimizing the detection and discrimination methodologies.

### 3.2.1 Regulatory levels for Radionuclide on Building Surfaces

Review of the and Code of Federal Regulations indicates the definition of the regulatory level for radionuclide contamination is somewhat clouded. Basee on our professional judgment a summary of current and relevant regulatory issues is provided.

NRC current policy is to proceed with decommissioning facilities on a site specific basis considering that residual radioactivity must be As Low As Reasonably Achievable (ALARA). Proposed amendments will provide specific radiological criteria, 15 millirem/year Total Effective Dose Equivalent (TEDE) for residual radioactivity distinguishable from background. Generic dose rate conversion factors are variable as well as computer model which provide site specific information for optimize the conversion factors for a specific site. An additional document provides a technical basis for gathering the necessary data for implementation of the residual contamination criteria.

Based on the generic dose rate conversion factors an estimated contamination in terms of instrument measurement can be calculated. These conversion factors are general for all radioisotopes.

The proposed ruling would require that site specific residual activity be substantiated using actual measurements to the maximum extent practical. Actual measurements reduces uncertainty associated with the modeling used to estimate TEDE to the average member of the critical group from residual radioactivity at the site. The critical group is defined as the group of

individuals reasonably expected to receive the greatest exposure to residual radioactivity given circumstances under which the analysis would be carried out. The actual measurements provide a greater measure of assurance that the radiological requirements are met.

### 3.2.2 Alpha Detection

The starting point for the alpha detection was Eberline's existing commercial product, the Alpha-6. This device is typically used in air monitoring application for discrimination of low levels of air borne alpha isotopes. The alpha isotopes are discriminated on the basis of pulse height using a multichannel analyzer determined from the penetration depth ( 'track') of the particle through the silicon substrate. The data are recorded as a function of energy in the multichannel analyzer. The discrimination is based upon "regions of interest" which are collection of channels summed together to give a response for a particular isotope. A one inch detector was integrated into the MSP. The associated electronics were integrated into the control software for the sensors.

### 3.2.3 Beta/Gamma Detection

The starting point for the beta/gamma technology was Eberline's Gas Proportional detector and modular detector board used in various commercial products. The gas (argon-carbon dioxide mixture) undergoes ionization by incident radiation. Charge is collected on the anode which is capacitively coupled to a comparator. Thresholds in the comparator discriminate noise and high energy alpha emission from the beta/gamma response. If gamma radiation is expected a 1/16" plate can be placed in front of the tube to discriminate it from the beta. A two inch diameter gas proportional tube was integrated into the MSP. The associated electronics were integrated into the control software for the sensors.

### 3.2.4 Experimental Results

The Phase II success criterion for the radionuclide measurement was met by detection of alpha activity at a level of 6 $Bq/cm^2$ from a thorium-230 standard at an signal to noise ratio of 37 in 40 seconds. In a previous test, at an appropriate facility, the beta sensitivity was determined to be 1 $Bq/cm^2$ or lower for a 10 second measurement time. Both the alpha and the beta sensors are capable of detection to regulatory levels[3,4,5] in less than one minute. These data show that the radionuclide sensor meets the Phase II success criteria of detecting radioactivity.

The experimental results for the multisensor probe include tests on functionality of the Radionuclide sensors, and integration of the CLR proximity sensor. The functionality and performance testing for the organic extraction and automated transport aspects of the multisensor probe was performed during Phase I and is expected to have similar performance in this Phase.

The tests included examination of the following:

- sensitivity for the radionuclide detectors,

- selectivity for the radionuclide detectors, and
- overall simultaneous function for the radionuclide and GC/MS.

Shown in Figure 3-11 is an example of the sensitivity testing for the alpha detector for materials embedded in concrete. The sample is thorium 230 embedded into concrete at 1 Bq/cm$^2$ level (the regulatory level). The data show that within 60 seconds on a rough concrete surface sufficient signal can be collected to identify thorium 230.

Shown in Figure 3-12 is the test data measured from standard samples of thorium, plutonium and americium. This experiment shows that sufficient resolution exists to differentiate these isotopes. No experiments were conducted on mixtures of these isotopes on concrete surfaces due to the difficulty of obtaining long term storage for the samples once the testing was completed. Based on the minor changes in the thorium standard and concrete samples it is expected that this sensor system will be capable of discriminating mixtures of these isotopes on concrete.

The radionuclide sensor was integrated with the robot controller. The data shown in Figure 3-13 is the alpha spectrum measured from a low level source at the Phase II demonstration. The corresponding GC/MS data are shown in Figures 3-3, 3-4, 3-5 and 3-6, and discussed in section 3.1.3. The solid trace is from the thorium source and the dotted trace is from a spot less than 2 inches away. The peak of the alpha spectrum is at an energy of 4.7 MeV indicating the sample is thorium-230. The alpha source is a sample of thorium-230 embedded ion a nickel substrate. These sources are typically used throughout the radiation health industries as check standards. During the demonstration the source was placed onto the concrete block near a organic contaminated spot. The MSP was positioned to 1 mm from the block and a simultaneous measurement of the organic and alpha sensors was made. The signal to background ratio is calculated to be 37 for the 40 second measurement time. This data indicate good alpha detection sensitivity.

Although the current configuration of the alpha sensor could not discriminate isotopes at level of 1 Bq/cm$^2$ in 40 seconds, a longer dwell time at the contaminated spot has shown that the isotope could be correctly identified. In operation, the measurement time of 40 seconds is sufficiently long to detect the presence of alpha activity at the regulatory level. A slightly longer time, approximately 180 seconds, is needed to discriminate at such a low level. At the regulatory level and speed of operation the alpha measurement is limited to detection only. Increasing the dwell time of the alpha sensor makes discrimination possible. The increased dwell time option for the alpha sensor will become part of the operational arsenal of the 3D-ICAS.

The beta activity sensor was demonstrated at an appropriate facility. The sensitivity is 1 Bq/cm$^2$ in a 10 second measurement time. The sensitivity of the gas proportional tube for beta and gamma detection was determined using different isotopes of widely varying activity (dpm). The data shown in Table 3-1 indicates an acceptable level of sensitivity for several beta emitting isotopes as measured in the background activity of the Eberline facility in New Mexico.

**Table 3-1. A summary of the Experimental Data Obtained in the Sensitivity Testing on the Beta Detector**

| Isotope | Current Activity (dpm) | Gross Count Rate | MDA* ($Bq/cm^2$) |
|---|---|---|---|
| SrY-90 | 5131 | 1080 | 0.414 |
| Ba-133 | 13114277 | 47300 | 23.1 |
| Tc-99 | 16320 | 4800 | 0.286 |
| Pm-147 | 8435 | 977 | 0.755 |
| C-14 | 4097 | 328 | 1.21 |

The final column of data is the 10 second minimum detected activity (MDA) at the 95% confidence level for the different isotopes using a 20 $cm^2$ detector area. These data indicate that the gas proportional tube is an effective detector for beta activity from surface as measured in air for short 10 second analysis times.

In Phase III, the alpha detector software will be modified for fastrer data transder allowing greater integration time for data collection. The hardware will be packaged in a smaller volume and hardened for field trials. The beta sensor will have limited broad band discrimination capabilities for selected isotopes, Cs, Co, Tc, Sr and Eu. The software will be modified for determination of the levels of these isotopes.

### 3.3 The Molecular Vibrational Sensor (MVS)

The sensor for identification of base materials of interest to DOE (concrete, transite, asbestos, wood, and other organics) is a combination of an IR reflection sensor and a Raman scattering sensor.

During Phase III, due to weight issues, the MVS probe will be based primarily on a near-infrared (NIR) spectrometer equipped with a silica fiber-optic probe and secondarily on a 785-nm Raman spectrometer equipped with a silica fiber-optic probe. High quality spectra have been obtained from most materials investigated within 1 to 2 minutes for both probes.

In an extensive test of a number of Raman spectrometers and laser wavelengths, it was shown that excitation at a wavelength of 785 nm gave the optimal combination of fluorescence rejection, minimal sample heating, portability and low data acquisition times to achieve a given signal-to-noise ratio (SNR). The Raman probe arrangement has been modified from the type studied in Phase I[6], in which the probe-head investigated incorporated 6 collection fibers around one excitation fiber (the so-called 6-around-1 arrangement) with no optical filtering. The optimum probe configuration was found to be a single input fiber with a filter mounted at the end

so that no Raman scattered radiation from the silica fiber reached the sample. The radiation scattered from the sample is then passed through a second optical filter to remove the Rayleigh-scattered light (at 785 nm) and pass all the longer-wavelength (Raman scattered) radiation which is then focused into a single output fiber. The second filter prevents the Rayleigh-scattered radiation from giving rise to Raman scattering in the output fiber. A highly sensitive and robust commercial spectrometer manufactured by Kaiser Optical Systems, Inc. was identified as being optimal for field analysis and a light weight probe from EIC Labs, Inc. for the measurement of the Raman spectra of solid samples with low Raman cross-section (such as asbestos). Early in Phase III an EIC Raman probe was adopted. This probe was found to be less sensitive than the Kaiser MkII probe but was cheaper and lighter. Low weight was necessary for the MVS sensor to be integrated with the MSP head of the 3D-ICAS system. This instrument is now in operation at the UI.

Two types of software for classification and identification of the samples have been studied. In the first, commonly known as spectral searching, the measured spectrum is compared directly to a library of reference spectra and the absolute difference between these spectra is calculated and summed over all wavelengths. The reference spectrum yielding the smallest sum is the best match to the spectrum of the unknown. This approach proves to be most useful when the spectrum of the unknown contains several narrow bands that are easily distinguished from the spectral baseline. In this case, an automated baseline correction routine that has been developed at UI can be applied prior to the application of the spectral searching program. For many of the samples, however, the spectra are not of the ideal form for spectral searching. For such samples, other approaches must be applied. Two such techniques were investigated in Phase II: a relatively well-known algorithm known as principal components analysis (PCA), and a new form of spectral classification involving the use of self-organized mapping (SOM) neural networks. The latter approach has proved to be more robust than either spectral searching or PCA and form the basis of the classification software in the final field version of the MVS probe. Other pattern recognition approaches are being reviewed in Phase III.

The results obtained with the silica fiber-optic probe analysis of the materials of DOE interest indicated that NIR diffuse reflectance (DR) spectrometry with a silica fiber-optic probe can be used to analyze all materials except those that totally absorb NIR radiation. It was also shown that NIR DR spectrometry could be used to distinguish between the five major types of asbestos. In Phase II it was shown that NIR detectors operating at room temperature did not allow for the spectral features that are important for distinguishing asbestos from analogous samples such as bricks and concretes to be extracted from the baseline noise). Recent advances in room temperature InGaAs detectors have allowed UI to use NIR DR to identify all the base materials with high reproductibility without the need to resort to the more expensive ENIR approach. The use of NIR DR also allows much longer sensor to spectometer distance and reduced MSP weight.

### 3.3.1 Near Infrared Spectrometry

A silica 7-around-1 fiber-optic probe for DR measurements coupled with a room temperature Indium Galium Arsinidf (InGaAs) detector has been purchased and interfaced to the ATI/Mattson Genesis Fourier Transform (FT) spectrometer. The system will cover the range

8000 - 4500 $cm^{-1.}$ The use of FT-NIR is necessitated since several materials have very sharp bands (full width at half height of 8$cm^{-1}$) in the NIR (especially asbestos). If classical low resolution dispersive NIR is used then these features are not observed and identification rates for asbestos are lowered. The combination of this probe and detector with the Mattson spectrometer enabled high quality spectra to be measured when the probe head was in direct contact with the sample. Typical spectra measured in 45 seconds will this instrument are shown in Figure 3-14.

For the fieldable NIR probe, direct surface contact is not permitted and thus the Visionex probe incorporates a bevel-tipped focusing arrangement allowing a 2.1 mm stand-off from the sample. This design may allow for small changes in the relative band intensities in the observed DR spectra. This effect can be accommodated by including appropriate reference spectra in the database for spectral identification or via software correction. The approach for this compensation is currently being determined.

Experimentally, we have shown that, for samples for which NIR DR spectra do not contain enough useful information to permit rapid identification, Raman spectrometry often does. Thus NIR DR and Raman spectrometry often prove to be highly complementary techniques.

### 3.3.2 Raman Spectrometry

Most CCD-Raman spectra were acquired on a Renishaw Raman spectrometer utilizing a microscope as the sampling device in Phase II. The 785-nm diode laser provided a maximum power of 2 mW at the sample. Excitation with gas lasers emitting at 632.8 and 514.5 nm was also tested but fluorescence overwhelmed the Raman spectrum features for most materials of interest. Different lenses allowed standoff distances between 1 and 10 mm to be tested. Single- and multiple-scan accumulation spectra were collected at approximately 6-$cm^{-1}$ resolution using CCD detector charge integration times from 1 to 120 seconds. Band positions are accurate to within 2 $cm^{-1}$. The results obtained with this spectrometer without the fiber-optic probe were sufficiently encouraging that we investigated other commercially available Raman spectrometers to which fiber-optic probes had been interfaced. Of these instruments, the one yielding spectra of solid samples with by far the highest SNR was the Kaiser Optical Holoprobe Raman spectrometer.

The Kaiser Holoprobe is a state-of-the art NIR Raman spectrometer optimized for use with 785-nm excitation. The system comprises a 300-mW external-cavity-stabilized diode laser providing a maximum laser power at the sample of greater than 100 mW, a transmission grating, a CCD detector, and a state-of-the-art fiber-optic probe packaged in a smaller volume than the Renishaw spectrometer. This system offered a usable Raman shift wavenumber range of 50 - 3500 $cm^{-1}$ with 785-nm excitation.

### 3.3.3 Tests for the Appropriate Excitation Wavelength

When the 632.8-nm and the 514.5-nm laser lines were used for excitation, the spectra are so severely affected by molecular and/or atomic luminescence that no Raman bands can be observed above the background. Thus the wavelength for the excitation laser for the MVS Raman probe had to be in the near infrared; in practice the only two wavelengths between which

a choice had to be made were 1064 and 785 nm. The 785 nm excitation was selected because of the greater strength of the Raman effect and shorter sample time required at that wavelength.

### 3.3.4 Probe-head Arrangements

The fiber-optic probe design for Raman spectrometry has changed significantly from the 6-around-1 arrangement tested in Phase I to the filtered probe-head now used.

The filtered probe-head arrangement prevents any Raman scattering from the fiber-optic cables from obscuring the Raman signal from the sample. The Kaiser Optical System[3] Raman probe was identified as optimal for the 3D-ICAS application based on the signal throughput of the fiber-probe, the low Raman cross-sections of some of the samples of interest in this project (especially, asbestos and concrete), the wavenumber range ($Æν$ = 50-1000 $cm^{-1}$) needed to identify DOE materials of interest. Recent requirements to limit the weight of the MSP head have caused UI to adopt an EIC probe head.

A recent study sponsored by the DOE at Westinghouse-Hanford[7] has shown for non-reflective non-fluorescent samples that a 6-around-1 probe-head with a flat-tip termination can yield up to an order of magnitude more signal than the filtered probe-head arrangement. It should be noted, however, that the filtered probe from EIC Labs had a lower throughput than the Kaiser MKII probe used in Phase II.

It has been shown both at the UI and in other DOE funded efforts[8,9] that if the background radiation caused by the Raman spectrum of silica in the input fiber is not filtered out the Raman signal from the sample can be significantly degraded or completely obscured. In Figure 3-15, the Raman spectrum of balsa wood measured through a 2-meter unfiltered 6-around-1 probe-head is presented. A comparison of the resultant balsa spectrum (Figure 3-15c) produced by subtraction of the silica background from the original probe-recorded spectrum of balsa with the balsa spectrum recorded in the macro-chamber of the spectrometer (Figure 3-15d) shows that the SNR has been significantly degraded when unfiltered fiber-optic probe-heads are used. This is especially obvious in the wavenumber range below 1000 cm-1 where spurious intensities for vibrational bands are observed between 200 and 1000 $cm^{-1}$. (It should be noted that Balsa wood is not a particularly weak Raman scatterer.)

In Figure 3-16 the Raman spectra of two asbestos minerals, chrysotile and crocidolite, are presented as well as the Raman silica background from the 2 meter 6-around-1 Raman probe. It can be seen that the silica background will obscure the strong vibrational bands of crocidolite (Figure 3-16b) and that the chrysotile bands may also be lost in the background. The asbestos minerals are very weak Raman scatterers (at least one order of magnitude weaker than the sample of balsa wood shown in Figure 3-15). Thus even though spectra measured with the 6-around-1 fiber-probe have not been obtained for the asbestos minerals it appears clear that the noise associated with silica background which is left in the resultant spectrum after background subtraction will totally obscure any asbestos signal from being observed.

In contrast, a filtered probe-head has been used to obtain Raman spectra of crocidolite within two minutes using only 5 mW of laser power; the signal level of these spectra is sufficient

to allow the mineral to be identified, as shown in Figures 3-17b and 3-17c. All the intense features in the reference spectrum (Figure 3-17, measured in about an hour) can be seen with a SNR of greater than 3 in spectra measured in 2 minutes with the fitted fiber-optic probe.

In conclusion since a number of materials of interest in this project (most importantly asbestos) possess crucial vibrational information in the region 800-50 $cm^{-1}$, the chisel-tip probe approach pioneered at Dow Chemicals and the flat-tip approach proved to be unsuitable for the DOE's specific needs. They have, therefore, not been adopted because both methods fail to meet the sample-dictated criteria necessary for routine analysis. The device based on the Kaiser Holoprobe Raman spectrometer with an EIC probe is the best available design (given the MSP weight and size constraints) for studies of weakly Raman scattering solid materials, especially when the wavenumber range below 800 $cm^{-1}$ is important (as it is for asbestos).

### 3.3.5 Software for Identification and Classification

Two types of software for classification and/or identification of the samples have been studied, spectral searching and self-organized mapping (SOM) neural networks. In spectral searching, the measured spectrum is compared directly to a library of reference spectra; the absolute difference between the spectrum of the unknown and each reference spectrum is calculated at each wavelength and summed over all wavelengths. The reference spectrum yielding the smallest sum is the best match to the spectrum of the unknown. Spectral searching proves to be most useful when the spectrum of the unknown contains several narrow bands that are easily distinguished from the spectral baseline. In this case, an automated baseline correction routine that has been developed at UI can be applied prior to the application of the spectral searching program.

Unfortunately, the spectra of many of the samples encountered in this project are not of the ideal form for spectral searching. For such samples two other techniques were investigated: principal components analysis (PCA), and self-organized mapping (SOM) neural networks. For both techniques, the dimensionality of the input date is reduced from a fairly large number (the number of data points in each spectrum, often several hundred) to a much smaller number (usually two). In each case, a two-dimensional plot is produced in which it is hoped that samples of a given type will form a cluster in a given region of the plot. In PCA, for example, the ordinates of the plot are the scores of the first two principal components (PC1 and PC2). When the ENIR spectra of a number of samples of brick, concrete, asbestos and polymers are subjected to the PCA, quite poor clustering results (Figure 3-18). With the use of SOM neural networks, on the other hand, most samples of a given type fell within well-defined regions of the map (Figure 3-19). Similar results were obtained with NIR spectra. Pattern recognition methods have proved to be more robust than either spectral searching or neural network computing and will form the basis of the classification software in Phase III.

## 3.4 3D-ICAS System Integration

The 3D-ICAS system uses its coherent laser radar (CLR) to obtain 3D facility maps, then uses the CLR to guide a robot arm borne multisensor probe along surfaces for contamination detection, 3D mapping and archiving. A substantial portion of the development effort has been devoted to obtaining the integrated functionality of these subsystems. We will describe some of these subsystems and their interaction briefly. We will then provide performance examples of the 3D-ICAS "eyes" the CLR 3D Mapper.

### 3.4.1 Robot Arm

Robot arm control and manipulation was an important part of the Phase II work. Integration of control of the robot arm shows advancement towards a fieldable system. During Phase II a model 465A robot arm from CRS Robotics (CRS) was selected, programmed and used to manipulate the sensor probe in a limited area.

The CRS 465A robot arm has about the same reach as a human's arm with more flexibility. The arm is not operated at full speed. The CRS C500 controller is programmed in the Robot Applied Programming Language, RAPL II, a language developed by CRS which is a derivative of BASIC and C. In Phase III the robot arm is being mounted on a mobile platform allowing for full working space access.

### 3.4.2 Multisensor Probe

The Phase II multisensor probe comprises the GC sensor head, two radionuclide sensors, one for alpha particles and one for beta/gamma emissions, and four proximity sensors. Three tetrahedron tracking targets are mounted on the outside of the probe. The probe is cube 6x6x6 inches and weighs 6 lbs.

The Phase III probe is essentially the same with two modifications. First, several tracking targets will be added to provide complete tracking capability. Second, the MVS sensor will be integrated with the other sensors on the probe.3.4.3 Proximity Sensor

The system uses commercial proximity sensors mounted at the four corners of the face of the probe. These proximity sensors provide a capability to move the probe up to a flat surface and maintain a standoff distance of 1 mm or more.

### 3.4.4 Robot Arm Platform

The Phase II system was not required to provide mobility for either the mapper or the robot arm. Portability was provided by mounting each unit on a wheeled tripod and moving them manually. For the Phase III demonstration the 3D-ICAS will take advantage of DOE developed mobility platforms for both the 3D mapper and the sensor robot arm.

### 3.4.5 Control Strategy

The multisensor probe moves to each point specified in the survey list in the order in which they appear in the list generated by the integrated workstation. Movement between points is along a standard sequence of steps. First, the multisensor probe moves from the rest position along a straight line to a position near the next survey point, rotating along the way so that the face of the probe is nearly parallel to the surface at the end of the segment. Second, the probe moves toward the surface until the proximity sensors detect the surface. The final approach is accomplished in small steps under control of the proximity sensors. The sensor system is commanded to acquire the contaminant sample and initiate processing. Then the probe moves along a straight line to the arm's rest position. When the probe has settled at each point, the CLR tracker is activated and a scan of the tracking target is made. The scan data are processed to provide an accurate estimate of the probe's location and orientation.

### 3.4.6 End Effector Tracking Function

CRC has developed an efficient approach for the CLR for tracking location and orientation of a robot end effector. Analysis, simulation, and laboratory experiments demonstrate the effectiveness of this technique. The tracking system has been integrated with the 3D-ICAS Phase II system demonstration. The tracker provides 6-DOF (X, Y, Z location and Yaw, Pitch, Roll orientation) tracking using a symmetric trihedral target.

### 3.4.7 Tracking Targets

The tracking target is a symmetric trihedron consisting of an equilateral triangle base and three identical faces. Reflective paint is applied to the entire target except along the edges between faces. Target size was constrained by the size of the probe and the face angle was selected considering location accuracy, orientation accuracy, and the number of targets required for full visibility.

### 3.4.8 Position Estimation Algorithm

The technique consists of scanning the CLR beam in a circular pattern around the apex of the target. The center and radius of the scan are preset so that the scan encircles the apex and remains on the target for the entire scan. Since the approximate location and orientation of the target are known, the desired scan pattern is easily determined. The CLR returns range, azimuth, elevation, and signal quality for each measurement point during the scan.

The first step of the position estimation algorithm is to estimate the three planes that best fit the three data sets independently. The intersection of the three planes determines the location of the apex of the target. The vectors normal to each plane are immediately available. These vectors provide the target's orientation. The second step is to fit the independent normal vectors by a set of normal vectors constrained in such a way that they correspond to a tetrahedron target with the specified face angle. The location of the apex is recomputed after the best fit orientation is determined. This estimate of location and orientation will be used as the starting point for a steepest descent optimization in Phase III.

### 3.4.9 Database Function

The database capability developed for the 3D-ICAS system serves as a repository for all of the data collected by the system. As the data are gathered, the system automatically sorts, keys and archives it for easy retrieval and display by the Integrated Workstation (IWOS). The data can also be made available for external clients as a server in an overall facility contamination management system.

Data are recorded for each survey point. The location of the sensor head is recorded precisely in facility coordinates along with the entire data structure from all of the sensors. The data structure includes raw data from the radionuclide (RN) and High-Speed Gas Chromatograph/Mass Spectrograph (HSGC/MS) sensors. Data from the Molecular Vibrational Spectrometer (MVS) is being incorporated during Phase III. The data structure also includes processed assignments for four organic compounds provided by the HSGC/MS. Finally the database holds any specific images generated from the raw 3D mapper data.

International Business Machine's (IBM) industrial database DB2 was selected for use in the 3D-ICAS system after surveying the leading large-scale commercial database vendors.

A primary consideration in the selection was the ability to directly support structured query language (SQL) in multi-platforms. SQL is used in the 3D-ICAS access and storage of the data. This allows future expansion of the system to provide the database information to other users in a networked environment. DB2 also runs on a wide variety of computers including workstations, PCS, and mainframes.

In 3D-ICAS DB2 will be run on the laser radar control computer. Using the preemptive multitasking capabilities of OS/2, the database will run in a separate session to ensure data integrity and responsiveness.

### 3.4.10 Data Archiving and Retrieval

The database is setup as a set of tables to store the following information (see Table 3-2):

**Table 3-2. Archival Data**

Identification

- Facility Identification (Agency, Plant, Building, Room)
- Date, time

Mapping

- Location of fiducial marks in room coordinate frame
- 3D mapper data in room coordinates
- Any generated facility scenes
- Bounding box of coordinates for each 3D mapping run

HSGC/MS

- 3D coordinates of each sample point (in room coordinates)
- Gas chromatogram for each point
- Mass spectrogram for each peak in each gas chromatogram
- Mass of each of five compounds at each point (PCB, fuel, volatile organics, explosives, other)

**Table 3-2. Archival Data (cont'd)**

RN

- 3D coordinates of each sample point (in room coordinates)
- Alpha spectrum
- Beta-Gamma count
- Activity level of each of six isotopes (U235, U238, Pu239, Pu242, Am241, Th230)

Queries can be made on all of the fields. The defined primary key fields used for sorting are the Facility Identification and Date, although any data field may be selected and sorted.

### 3.4.11 Data Display: Facility Scene

A facility scene image is generated from the 3D facility frame mapper data by selecting the area to display and an optical viewpoint and converting range from the viewpoint into a rendered image. The facility scene is rendered in black and white so that subsequent contamination overlays in color will be highlighted.

### 3.4.12 Data Display: Contaminants

When a facility scene is displayed on the IWOS, the database can be queried for related survey information. The data can be overlaid on the facility scene as scatter contour plots or displayed in one of several different graphical or list windows.

Contaminant concentration levels are presented as thresholded scatter diagrams rather than continuous line contour plots because the interpolation ingerent in constructing continuous contours could produce an erroneous picture of the contamination, especially when the survey points are widely separated. Each contaminant is displayed in its own window. The window contains the gray scale facility scene overlayed with contamination levels in color. An asterisk is placed at each location where a measurement was made. The color of the asterisk depends on the concentration of the contaminant. Green, yellow, red, and blue indicate no, light, medium, and heavy contamination respectively. Default thresholds for defining the four contamination levels are provided; the user may change the thresholds.

More detailed displays of contamination data are keyed from the facility scenes with contamination overlays on them. For any contamination display, the operator can select a location to get detailed information about with the mouse. Radionuclide activity levels are displayed in tabular form. Gas chromatograms are displayed in graphical form. Masses of the five organic compounds are displayed as a bar graph. Secondary displays consisting of mass spectrograms are obtained by mousing on desired peaks in the gas chromatogram; mass spectrograms are displayed as graphs and also in tabular form.

# 4.0 Application and Benefits

The completed 3D-ICAS will be directly applicable as a system to DOE facility characterization decontamination and decommissioning. The sensor subsystems of 3D-ICAS represent an advance in portable real-time chemical analysis for chemical constituents and dangerous materials of interest to DOE. The CLR 3D mapping subsystem, developed outside of the 3D-ICAS program, can perform as a critical subsystem on a wide range of DOE robotic applications and I industrial metrology applications.

Benefits of 3D-ICAS High Speed Contaminant/Base Material Analysis for Overall Decontamination and Decommissioning Operations

3D-ICAS site chemical analysis is expected to improve the technological capabilities of current chemical analysis methods by combining state-of-the-art sample preparation techniques, High Speed GC, time-of-flight mass spectrometry (TOF-MS), molecular vibrational spectrometry, and radionuclide analysis into a system that can be operated at a field site to provide real-time, reliable qualitative and quantitative results. The availability of this technology will positively impact DOE clean-up operations in the following ways:

- Improved Performance (faster, more accurate)
- Cost Reduction
- Reduction of Health Risks
- Reduction of Environmental Risk
- Improved Operations
- Waste Minimization

**Improved Performance**: The quality of analytical data generated by 3D-ICAS chemical analysis instrumentation will equal or exceed that currently being generated by conventional laboratories. Sample automation and elimination of the extensive sample handling associated with off-site storage and analysis will improve the reliability of the data as well as significantly reduce sample preparation time. High speed GC techniques will produce chromatographic peaks more than 100 times sharper than conventional separations and improve the detector performance for a given mass of analyte. High speed GC will also reduce the separation time from 20-45 min for a typical run down to 100 seconds or less, resulting in faster analysis times. The Radionuclide analysis may not provide more sensitivity than conventional laboratory analysis, but the direct real-time field results will certainly produce the required data expeditiously. Molecular vibrational spectrometric analysis will identify inorganic and organic surface materials and moderate (down to low parts per million) levels of contaminations, at high spatial resolution, in sample times as short as five seconds.

**Cost Reduction**: The proposed technology will reduce the overall cost of clean-up operations. Costs for chemical analysis will be reduced because the whole process from sample preparation to data management can be automated and performed on-site. Operational cost benefits will result from the availability of real-time analysis. Manpower and equipment costs

would be reduced through the use of the robot operated chemical instrumentation due to improved operational efficiency.

**Reduction of Health Risks**: The automation of sample preparation steps and actual site mapping would eliminate sample handling by laboratory personnel. Further, survey worker exposure to hazardous locations would be significantly reduced or eliminated. Insurance premiums alone will be reduced (it should be cheaper to insure robots than workers).

**Reduction of Environmental Risks**: On-site, real-time analysis with the robot operated analyzer would provide improved site monitoring during decontamination. Using teal-time analysis, engineers could monitor and respond to problems in less time than is possible with conventional chemical analysis.

**Improved Operations**: The robot operated analysis instrumentation would improve the capabilities of DOE response in each of the three phases of remedial efforts by providing a more efficient, streamlined beginning-to-end operational capability. During the survey state worker exposure is reduced; and mapping and characterization efforts proceed efficiently with the aid of real-time, remote controlled mapping and analysis. For example, when mapping out the contaminated area, engineers could review analytical results immediately and direct more intensive efforts where they are needed most. More accurate and detailed characterization of the waste site would concentrate restoration efforts to contaminated areas and eliminate needless efforts on areas that are in compliance or pose minimum risk. Once decontamination efforts are begun, removed materials and remaining site locations could be continually monitored to measure the progress of clean-up operations. Remediation operations would proceed faster because field engineers could have near real-time results indicating the status with respect to regulatory requirements.

**Waste Minimization**: Real-time monitoring of decontamination operations would have a direct impact on the amount of waste generated during remediation. Procedures could be halted as soon as compliance is achieved, preventing excess of removal of otherwise clean material. More detailed mapping and characterization of site would identify areas that are in compliance and do not require decontamination. The analyses would be able to classify materials as they are removed thus optimizing the handling requirements to be consistent with their hazard level.

**CLR 3D Mapper Advantages over all Other Current Technologies**

**Immunity to Ambient Light and Surface Shading**: The FM CLR is immune to ambient lighting conditions in an exactly analogous way that FM radio is immune to the background amplitude bursts in lightning. The other methods depend upon amplitude detection.

**Lightweight Radiation Resistant Fiber Optic Implementation**: The high sensitivity of the FM CLR detection process allows the use of a remote scanner at the end of an optical fiber with no solid state electronics. Because of the high efficiency of the optical fibers, the remote scanner could, in principle, be kilometers from the integrated workstation.

**Benefits of the CLR 3D Mapper Performance Advantage**: The fast CLR 3D Mapping capability will not impede or interrupt D&D operations. Immunity to lighting conditions means that other D&D operations will not have to be disrupted while lighting is controlled for 3D mapping operations. A more accurate 3D mapping capability allows robotic operations to proceed with less supervision for characterization, decontamination, and dismantling operations. Characterization benefits from the high accuracy CLR 3D mapping are:

- Allows clear visualization of surface and more accurate planning and execution of surface contaminant mapping operations
- Allows the sensor probe to follow a surface at close proximity without collision
- Supports object shape and texture determination and better contaminant penetration modeling

## 5.0 Future Developments

The Phase III 3D-ICAS development is aimed at demonstrating an fieldable contamination 3D mapping, analysis and archiving system to support D&D operations. Highlights of the 3D-ICAS system capability and performance improvements to be accomplished in Phase III are as follows:

- Integration of the multisensor probe and supporting robot arm 3D-ICAS sensor subsystem) with a DOD provided mobility platform
- Integration of the CLR 3D Mapper subsystem with a DOE provided mobility platform
- Reduction in size and weight and field hardening of sensor subsystems and analysis hardware
- Improvement in speed of the CLR guided 6DOF multisensor probe end effector tracking and control
- Increase in flexibility of sensor route planning to allow a variety of mapping coverages for each sensor component
- Refinement of contaminant detection and analysis software for all sensor components
- Refinement of system control, display, and other human interface software
- Adaptation of 3D-ICAS system mission to evolving DOE site cleanup requirements

## 6.0 References


1. EPA 40 CFR Part 761 Polychlorinated Biphenyls Spill Cleanup Policy 52 FR 10688 April 2, 1987.

2. 59 FR 62788 Disposal of PCBs vol. 59, No. 233, part II Dec. 6, 1994.

3. Technical Basis Document, "Residual Radioactive Contamination from Decommissioning: Technical Basis for Translating Contamination Level to Annual TEDE" (NUREG/CR- 5512).

4. "Guidance for Conducting Radiological Surveys in Support of License Termination" (NUREG/CR-5849)

5. 10 CFR Part 20 Radiological Criteria for Decommissioning; Proposed Rule a)

6. Phase I Topical Report to DOE. 1994. 3-Dimensional Integrated Characterization and Archiving System (3D-ICAS).

7. T. Lopez, F.R. Reich, and J.G. Douglas. Summary of FY 1994. Raman Spectroscopy Technology Cold Test Activities Document, US DOE Contract DE-AC06-87RL10930, 4-8 (1995) available as Westinghouse-Hanford Document WHC-SE-WM-RPT-116, Westinghouse-Hanford, Richland, Washington.

8. K.P.J. Williams, J. Raman Spectrosc., 21 147 (1990).

9. J. Sawatski, Proc.XIII Internatinal Conference on Raman Spectroscopy (ICORS XIII), Eds. W. Keifer, G. Schaack, F.W. Schneider, and H.W. Schrotter, Additional Presentations Volume, Wiley, Chichester (1992).

10. T.F. Cooney, H.T. Skinner, and S.M. Angel. 1995. Personal Communication.

11. R.D. McLachlan, G.L. Jewett, and J.C. Evans. 1986. (Dow Chemical Co., Midland, MI), Fiber-Optic Probe for Sensitive Raman Analysis, US Patent 453771.

## Acknowledgements

This development is supported by the Department of Energy under contract DE-AC31-93MC30176. Dr. V.P. Kothari is the METC COR. Period of performance is 9/30/94 to 9/1/97. The MVS is being developed by University of Idaho under subcontract with Coleman Research Corporation. The sensors for organics and radionuclides are being developed by Thermedics Detection, Inc., under subcontract with Coleman Research Corporation.

## Acronyms

| | |
|---|---|
| 3D | Three Dimensional |
| 3D-ICAS | Three Dimensional Characterization and Archiving System |
| 6-DOF | six degrees of freedom |
| ALARA | As Low As Reasonably Achievable |
| amu | atomic mass units |
| CLR | coherent laser radar |
| CRS | CRS Robotics |
| D&D | Decontamination and Decommissioning |
| DB2 | database program |
| dpm | disintegrations per minute |
| DOE | Department of Energy |
| DR | diffuse reflectance |
| ENIR | extended NIR |
| FT | Fourier Transform |
| GC | Gas Chromatograph |
| GC/MS | gas chromatographs-mass spectrometer |
| HSGC/MS | High Speed Gas Chromatograph/Mass Spectrometer |
| IBM | International Business Machines |
| IR | Infrared |
| IWOS | Integrated Workstation |
| Mb/second | megabits per second |
| MS | Mass spectrometer |

| | |
|---|---|
| MSP | Multisensor Probe |
| MVS | Molecular Vibrational Sensor |
| NIR | near IR |
| NIST | National Institutes of Standards and Technology |
| NRC | Nuclear Regulatory Commission |
| OS/2 | Operating system/2 |
| PCA | principal components analysis |
| PCB | polychlorinated biphenyl |
| RAPL | Robot Applied Programming Language |
| RF | Radio frequency |
| RN | Radionuclide |
| SNR | signal-to-noise ratio |
| SOM | self-organized mapping |
| SQL | structured quiery language |
| TCP/IP | Interface protocol |
| TDI | Thermedics Detection, Inc. |
| TEDE | Total Effective Dose Equivalent |
| TOF-MS | time-of-flight mass spectrometer |
| UI | University of Idaho |

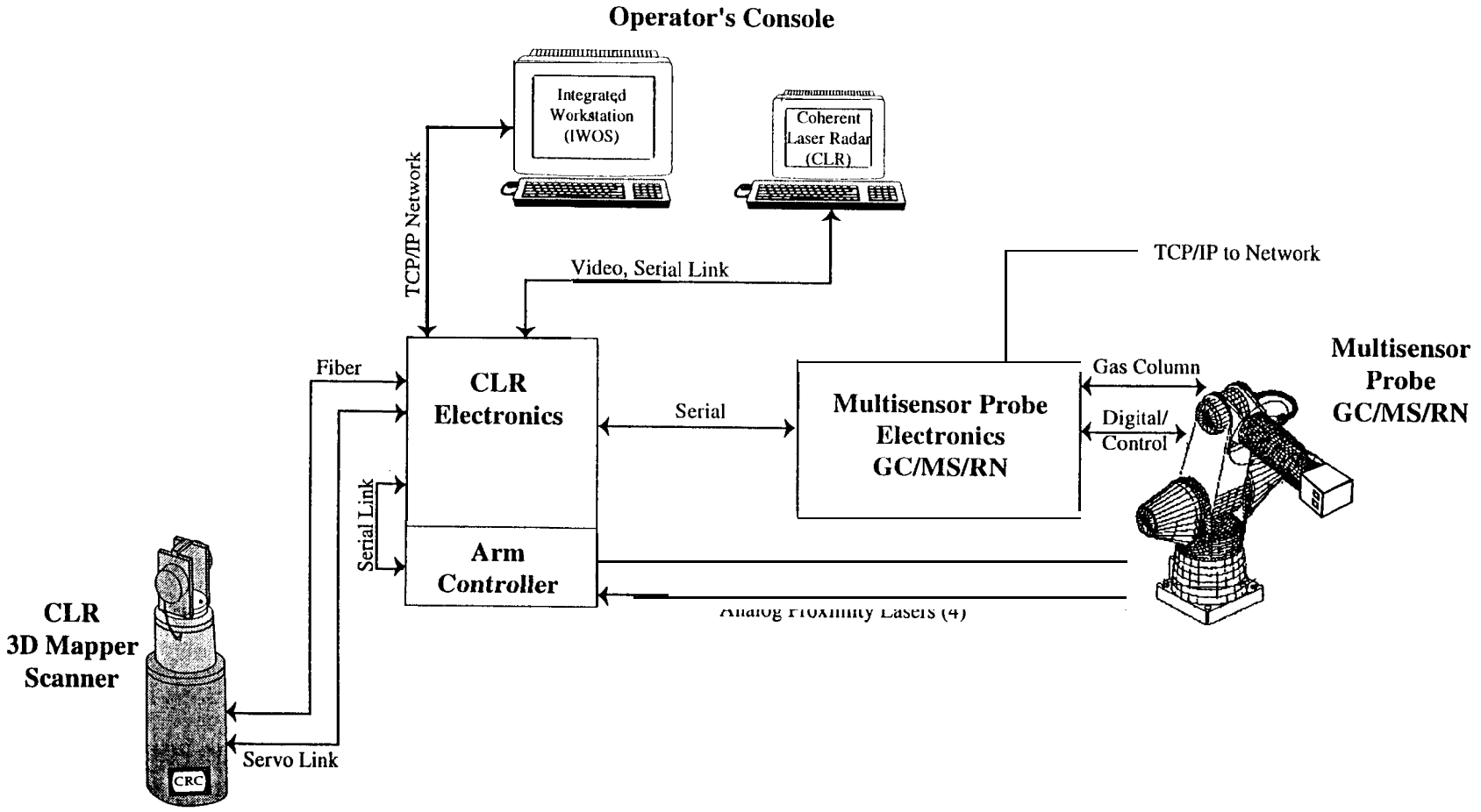


Figure 2-1. 3D-ICAS Phase I Block Diagram

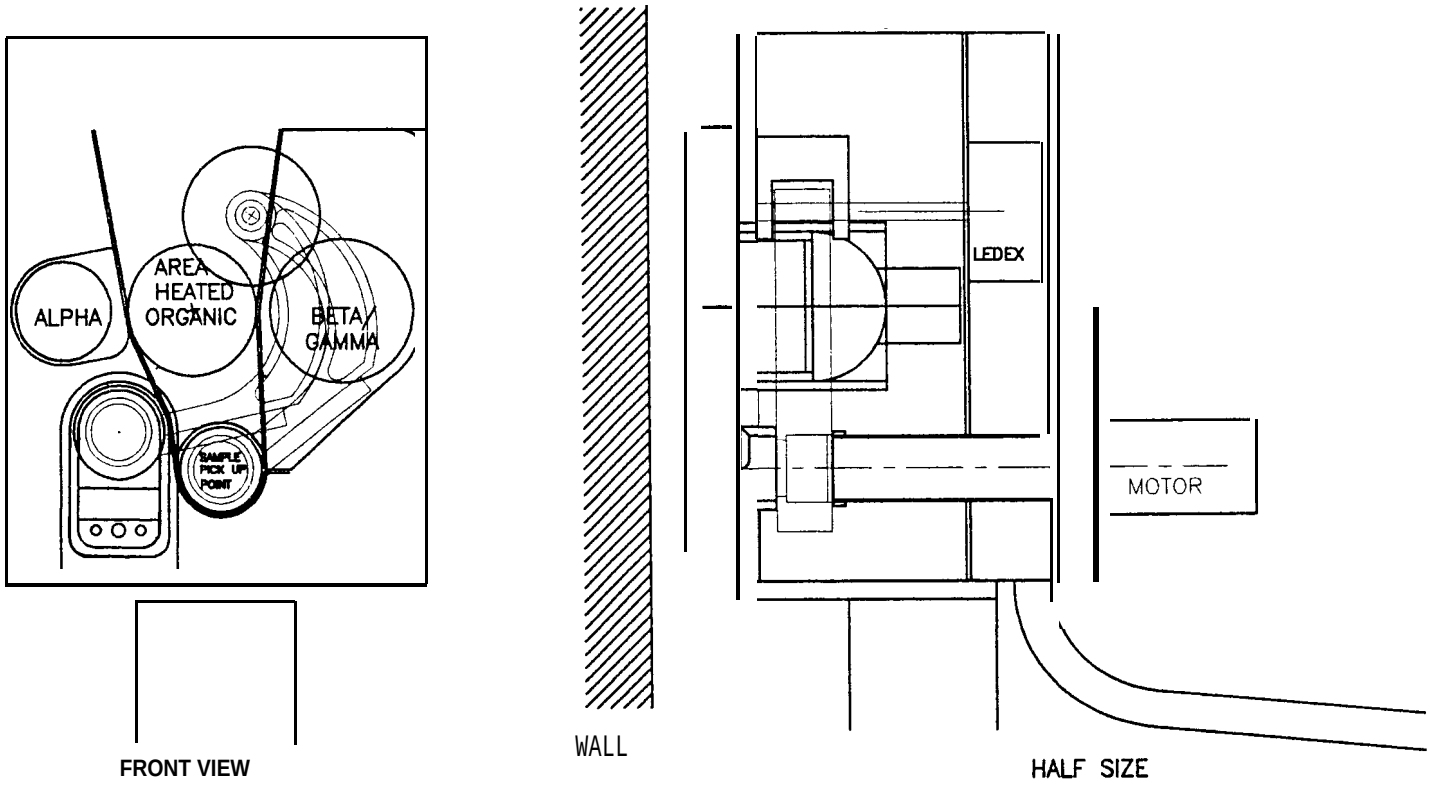


**Figure 2-2. Diagram of Multisensor Probe Design used During Phase H**

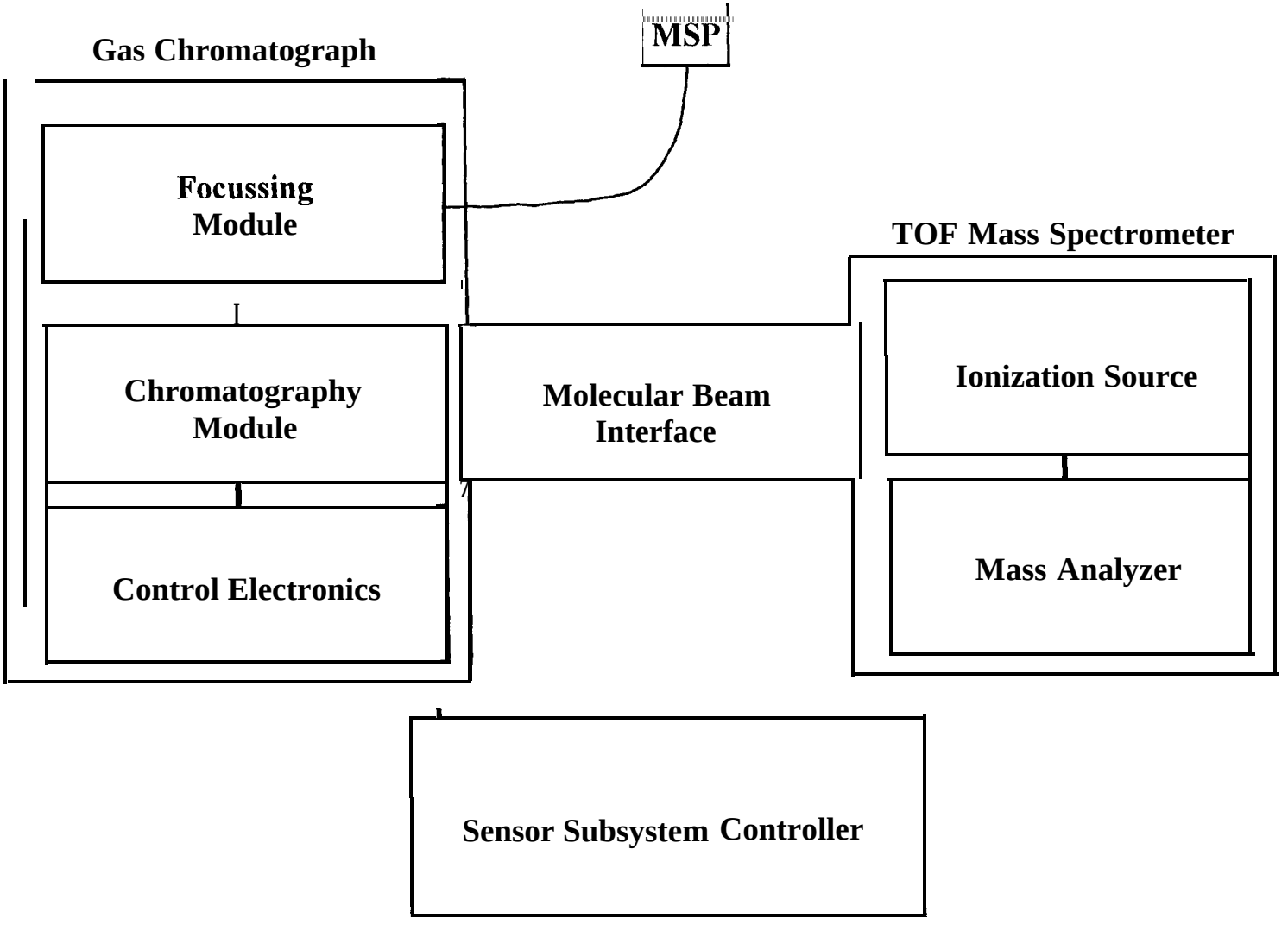


**Figure 3-1 HSGC/MS Block Diagram**

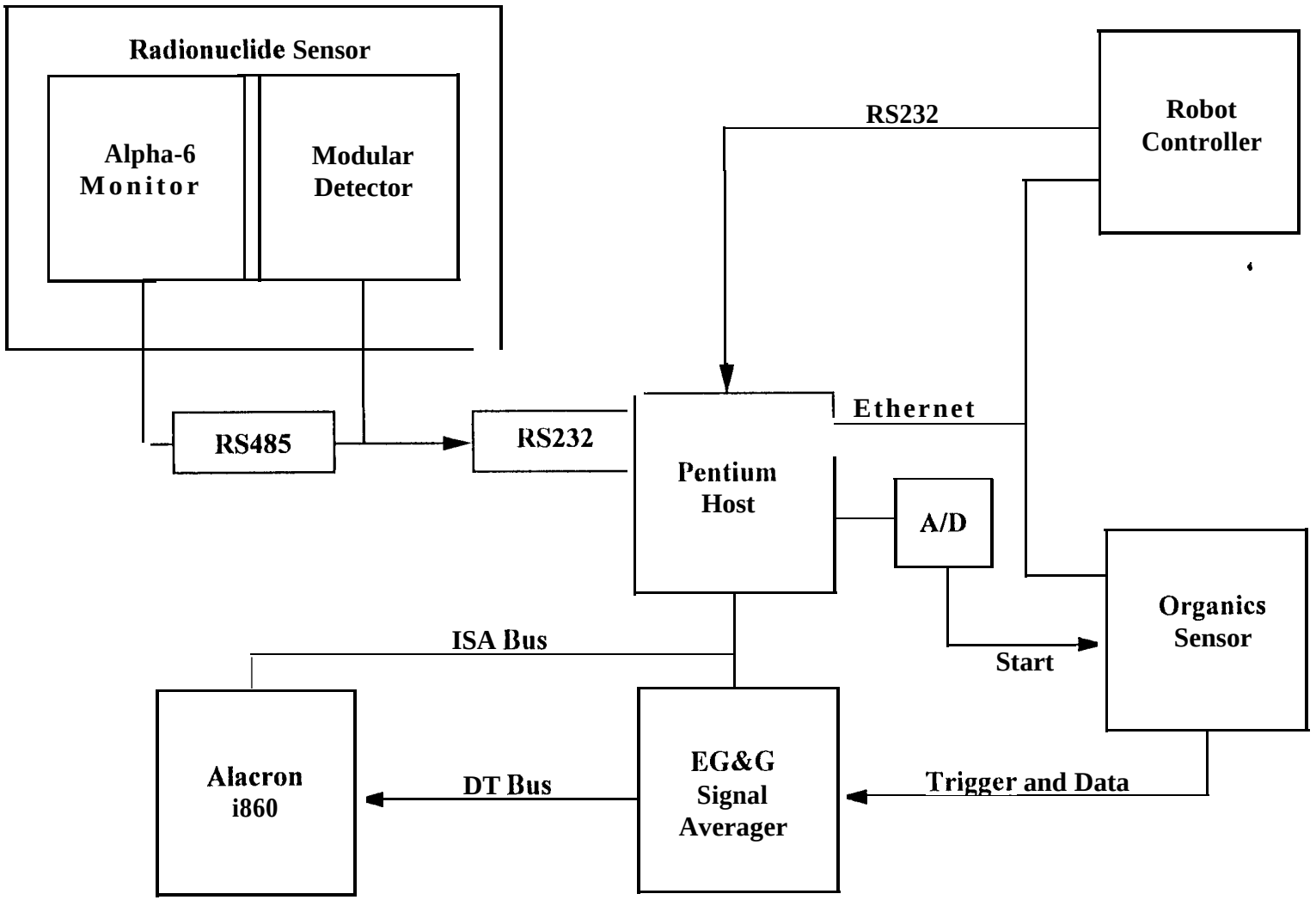


**Figure 3-2 HSGC/MS Data Acquisition System**

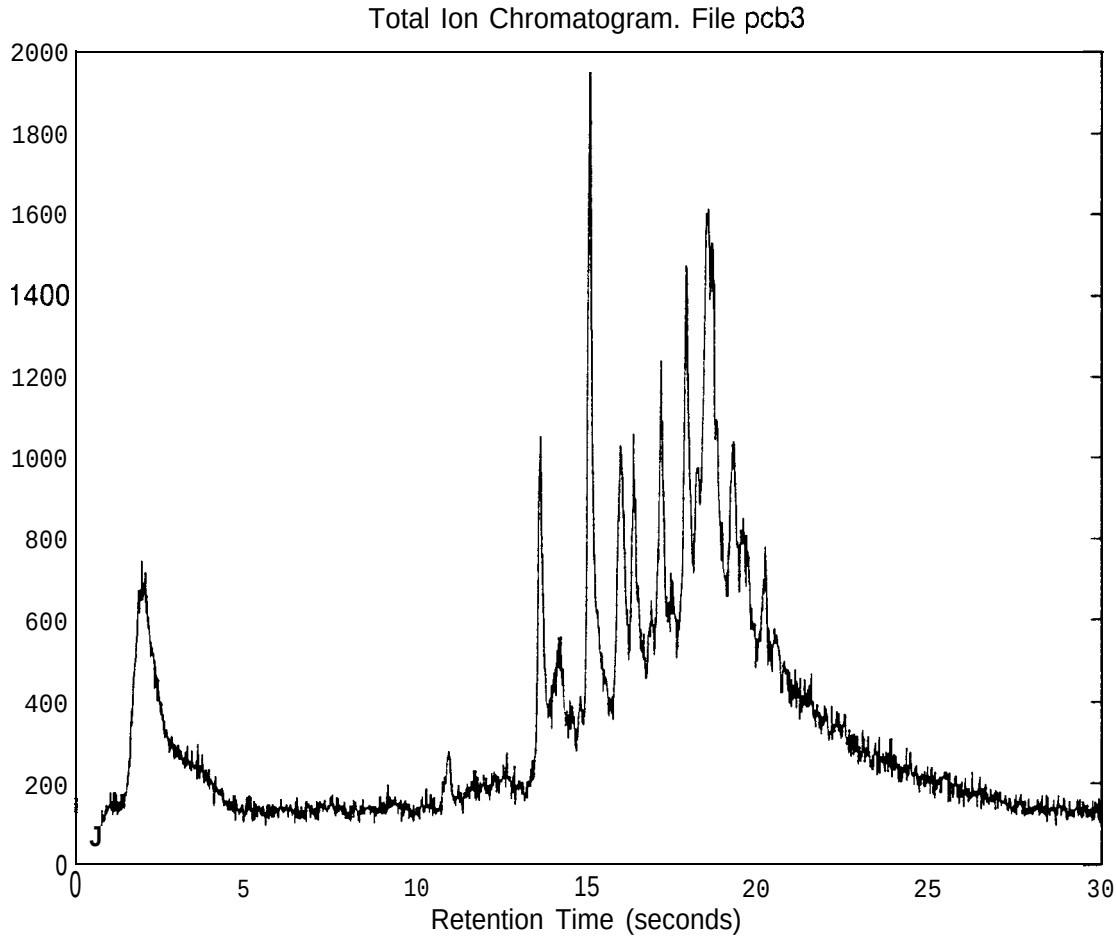


**Figure 3-3. Total Ion Chromatogram 4µg/10cm$^2$ PCB Mixture**

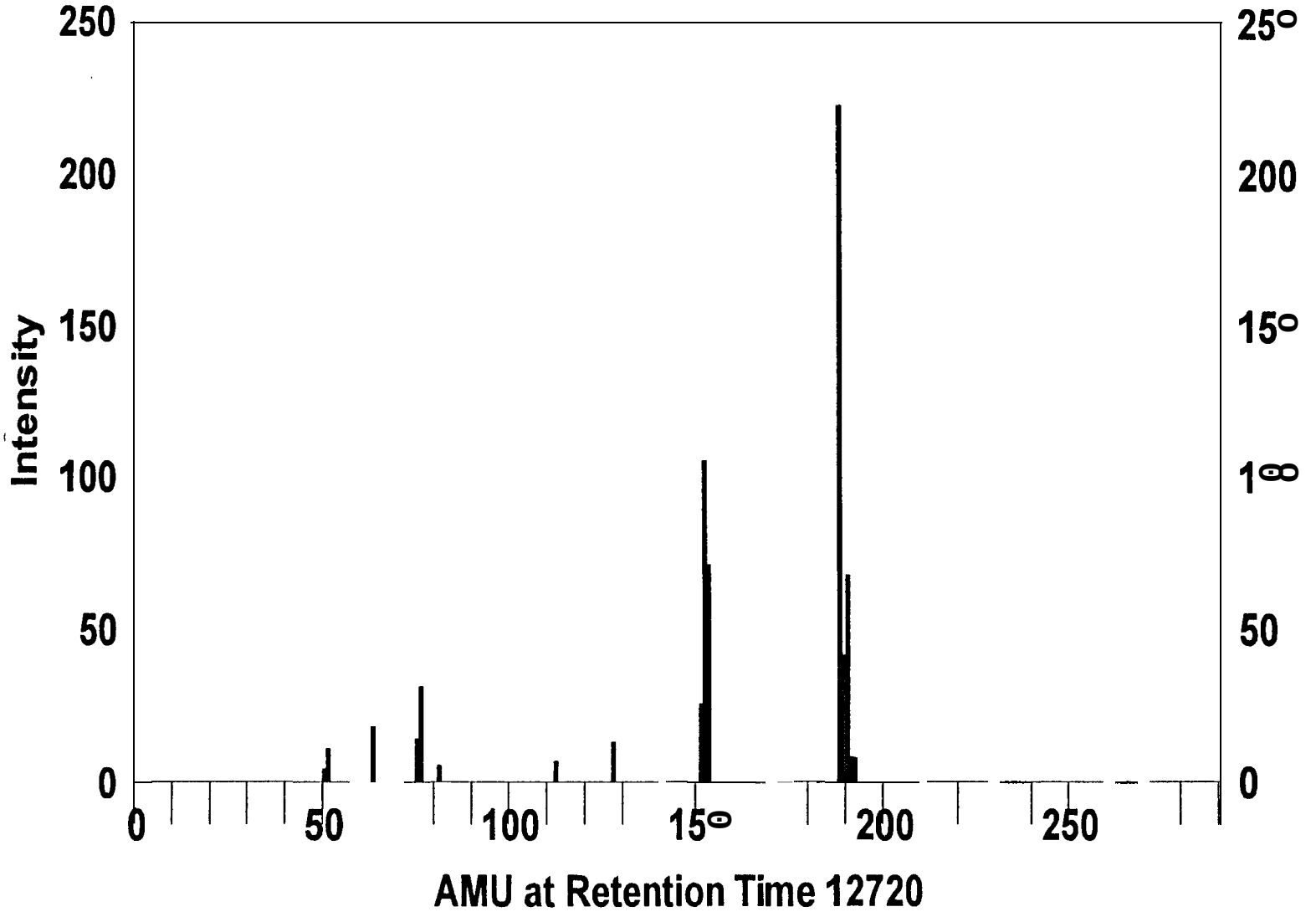


Figure 3-4. Mass Spectrum Meausred at 2.720 Seconds Identified as Chlorobipheny using NIST MS Database

| Peak At | Confidence | Compound | Class | Quantity |
|---|---|---|---|---|
| 11200 ms | 26.17% | Hexane, 2,2,3,3 -tetramethyl- | Voc | 285.96 ng |
| | 21 .09% | Pentane, 3-ethyl-2,3 -dimethyl- | | |
| | 12.78% | Nonane, 2,5-dimethyl- | | |
| | 7.74% | Heptane, 4-ethyl- | | |
| | 6.24% | 4,4-Dipropylheptane | | |
| 11216 ms | 42.72% | Benzene, (2,4-cyclopentadien-1-yl | Fuel | 227.70 ng |
| | 34.43% | Biphenyl | | |
| | 1 0 . 5 % | Naphthalene, 2-ethenyl- | | |
| 12672 ms | 27.66% | 1(2H)-Pyrazineacetamide, 5-amin | Other | 396.82 ng |
| | 16.76% | 2,4( 1 H,3H)-Pyrimidinedione, dime | | |
| | 13.51% | 1,4-0 ioxaspiro[4.5]decane, 8-met | | |
| | 10.89% | Uracil | | |
| | 6.6% | 2-Butenediamide, 2-methyl-, (Z)- | | |
| 12720 ms | 85.64% | Biphenyl, chloro- | PCB | 433.45 ng |
| 13520 ms | 70.62% | Biphenyl, monochloro- | PCB | 125.04 ng |
| | 5.69% | Propanedinitrile,[(2-chlorophenyl) | | |
| | 4.59% | Chloralose | | |
| 13968 ms | 72.63% | Biphenyl, dichloro- | PCB | 261.57 ng |
| 14816 ms | 66.38% | Biphenyl, chloro- | PCB | 337.62 ng |
| 14800 ms | 73.98% | Biphenyl, dichloro- | PCB | 296.16 ng |
| 15488 ms | 69.96% | Biphenyl, trichloro- | PCB | 529.61 ng |
| 15856 ms | 42.22% | Silane, diethoxydiphenyl- | Fuel | 211.18 ng |
| | 25.58% | Allobarbital 1,2(or 4)-dimethyl der | | |
| | 7.8% | [1, 1'-Biphenyl]-2-amine, N-(1 -met | | |
| | 4.72% | 1,3,5 -Triethylcyclotrisiloxane | | |
| 16208 ms | 37.26% | Biphenyl, dichloro- | PCB | 244.49 ng |
| | 23.12% | Thiourea, N-pentyl-N'-phenyl- | | |
| | 9.1% | Benzene, 1,3,5-trichloro-2,4,6-tri | | |
| 16288 ms | 78.13% | Biphenyl, trichloro- | PCB | 563.30 ng |
| I 6880 ms | 68.27% | Biphenyl, tetrachloro- | PCB | 271.48 ng |
| 17760 ms | 76.31 % | Biphenyl, tetrachloro- | PCB | 146.94 ng |
| 17792 ms | 65.96% | Biphenyl, tetrachloro- | PCB | 184.41 ng |

**Figure 3-5. Detailed Listing of Organic Data Generated from GC/MS Measurement**

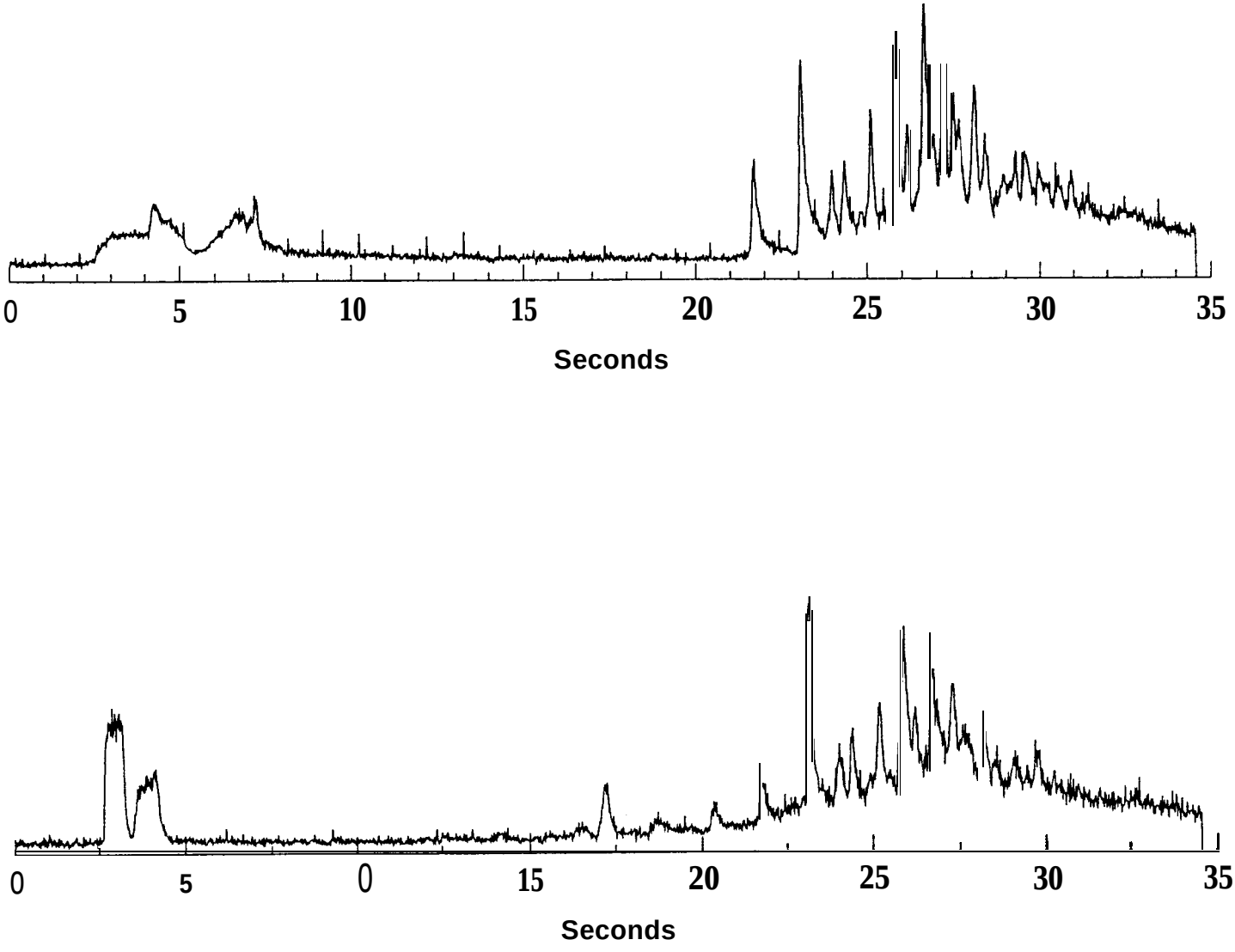


**Figure 3-6. PCBS Analyzed from a Syringe Injection (upper) and Thermal Extraction (lower) using the Multisensor Probe**

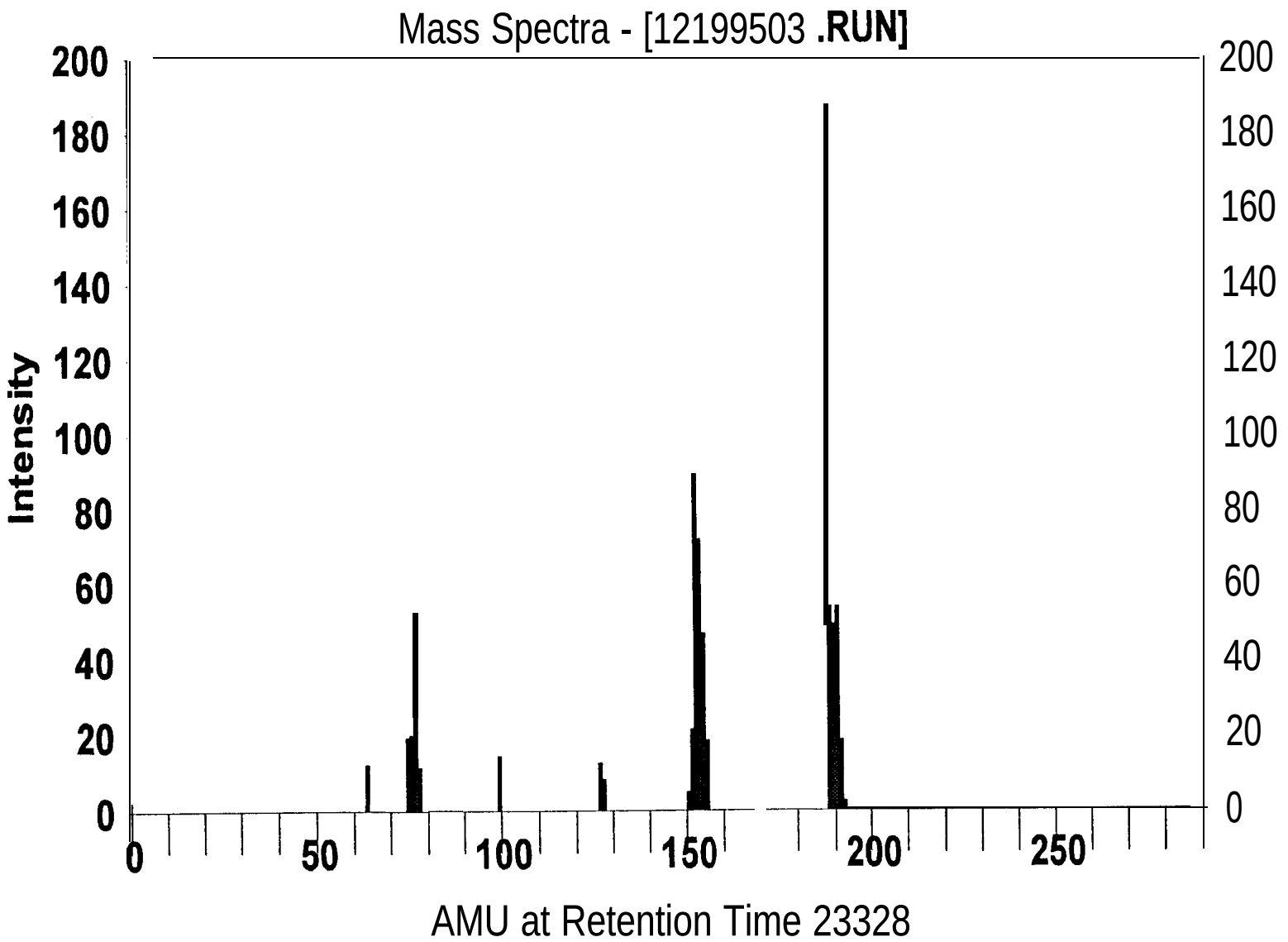


**Figure 3-7. Mass Spectrum of Chlorobiphenyl as Measured from Syringe Injection**

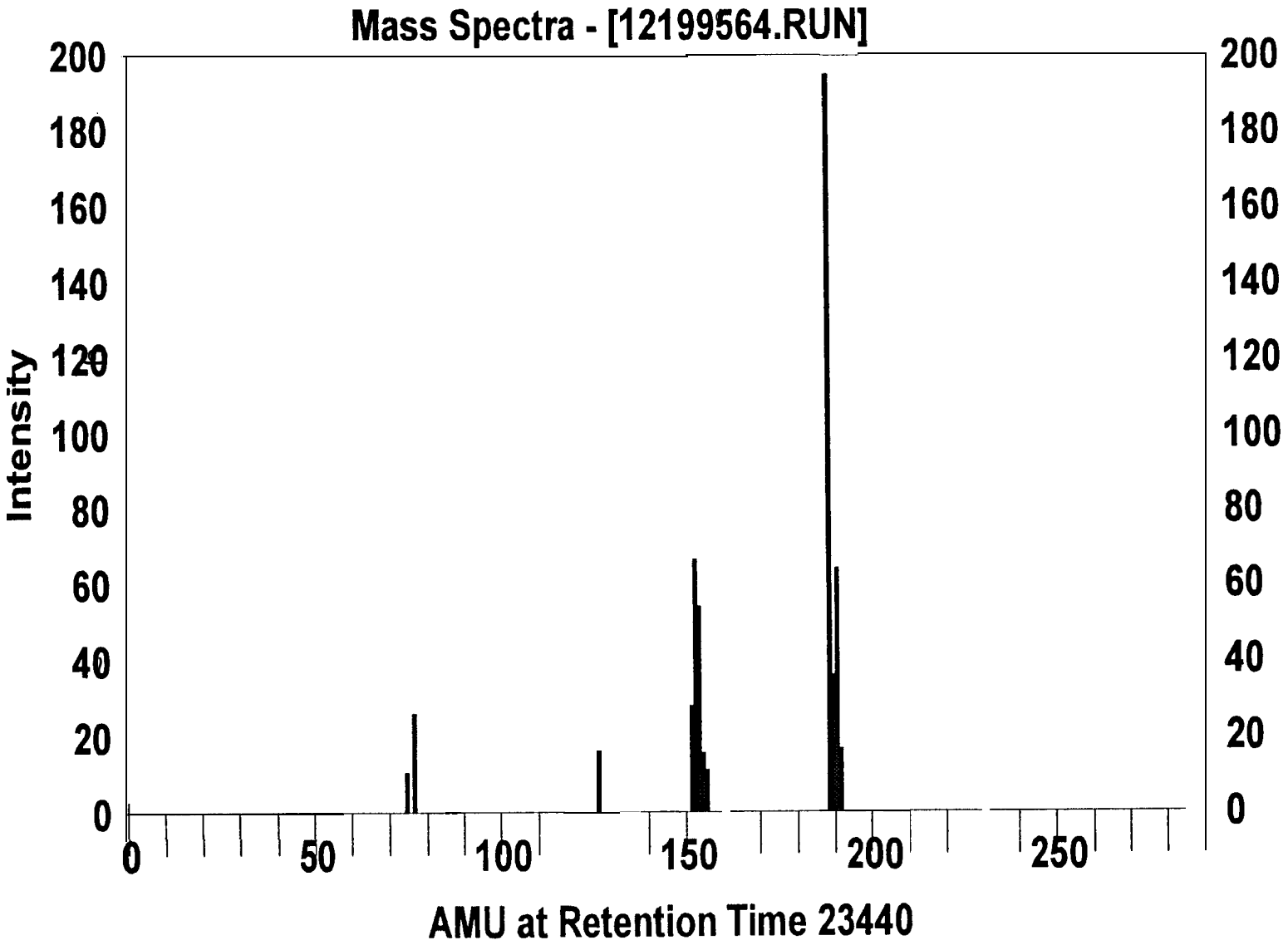


Figure 3-8. Mass Spectrum of Chlorobiphenyl as Measured from Thermal Extraction

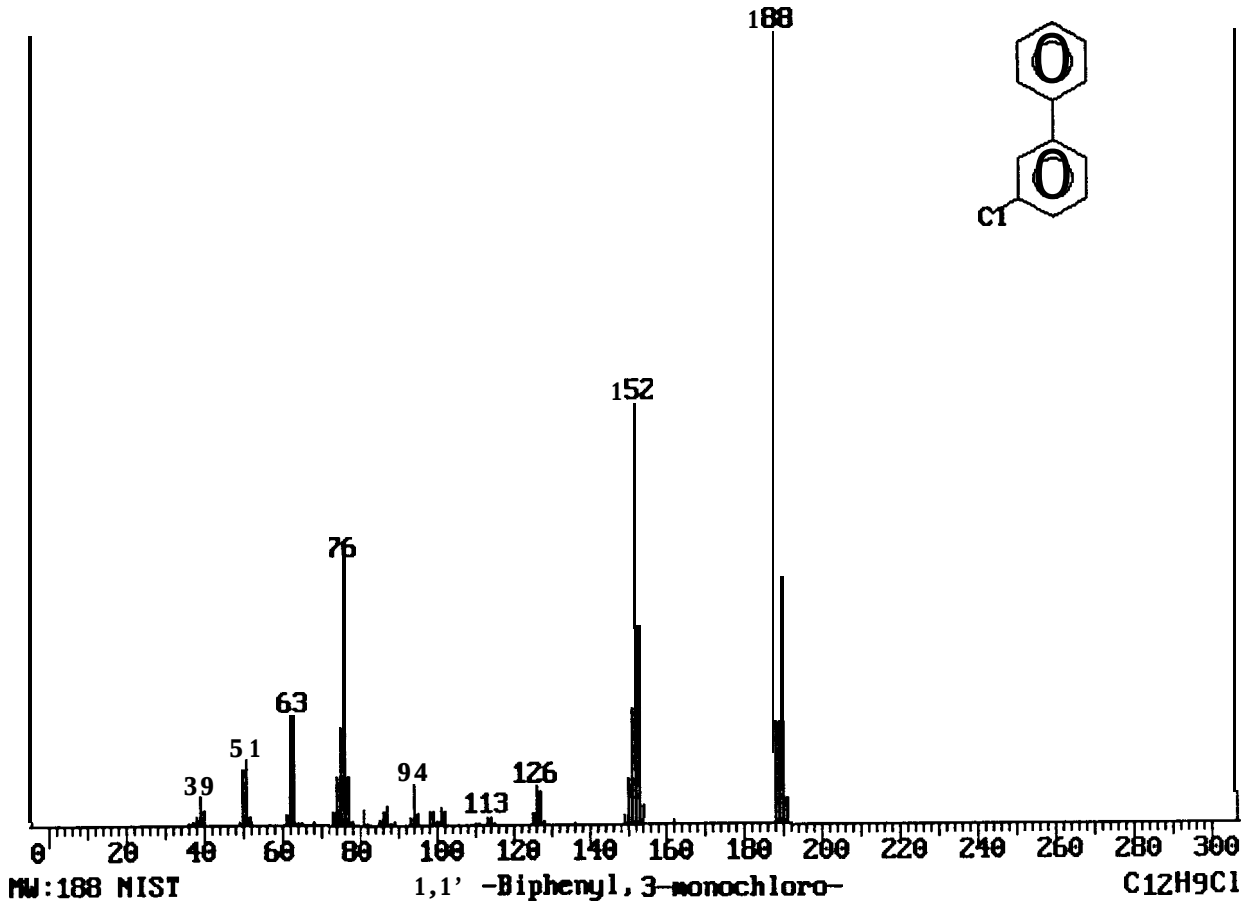


Figure 3-9. Mass Spectrum of Chlorobiphenyl from the NIST Database

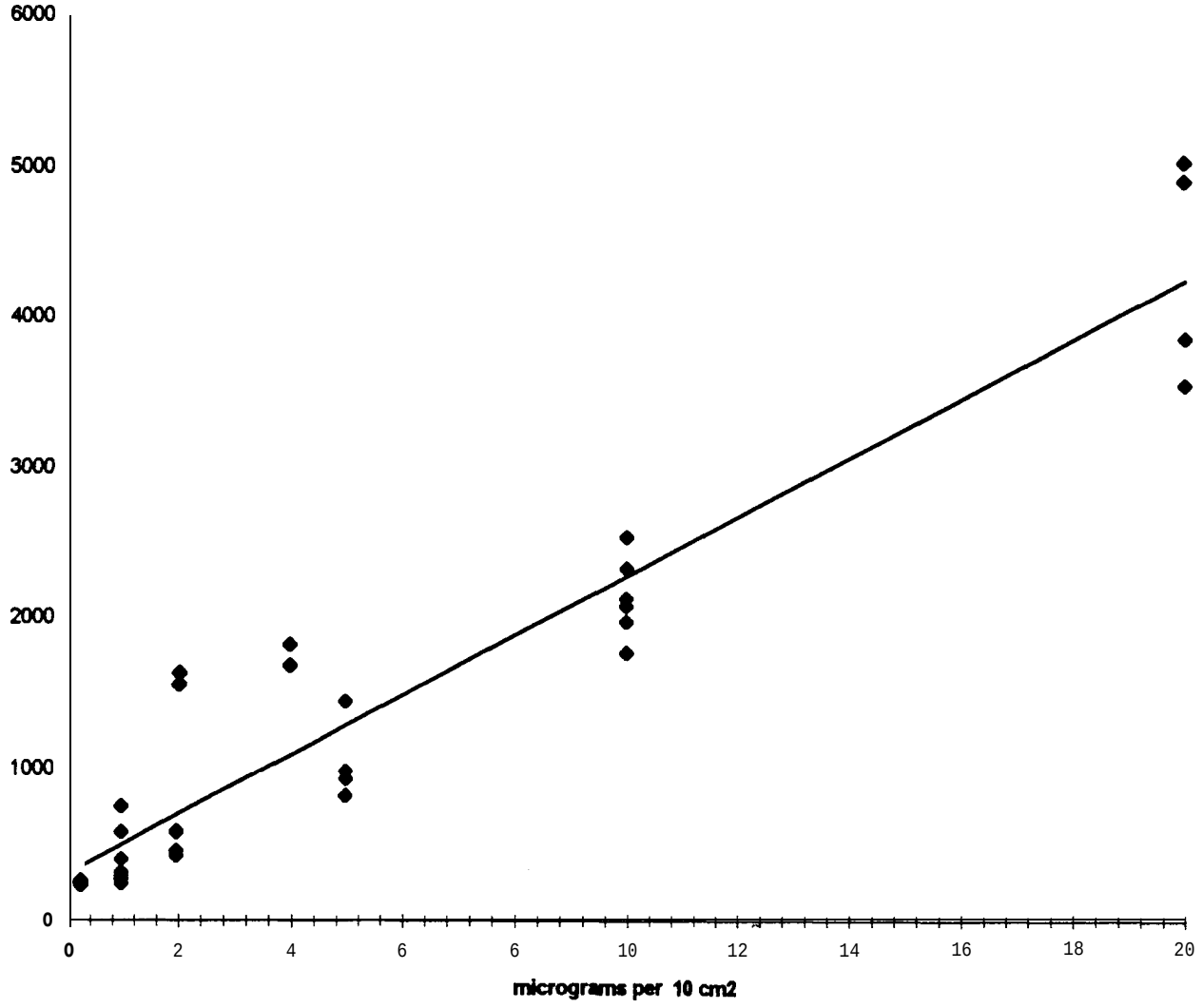


**Figure 3-10. Calibration Curve for the High Speed GC/MS Analysis of PCB Thermally Extracted from Concrete**

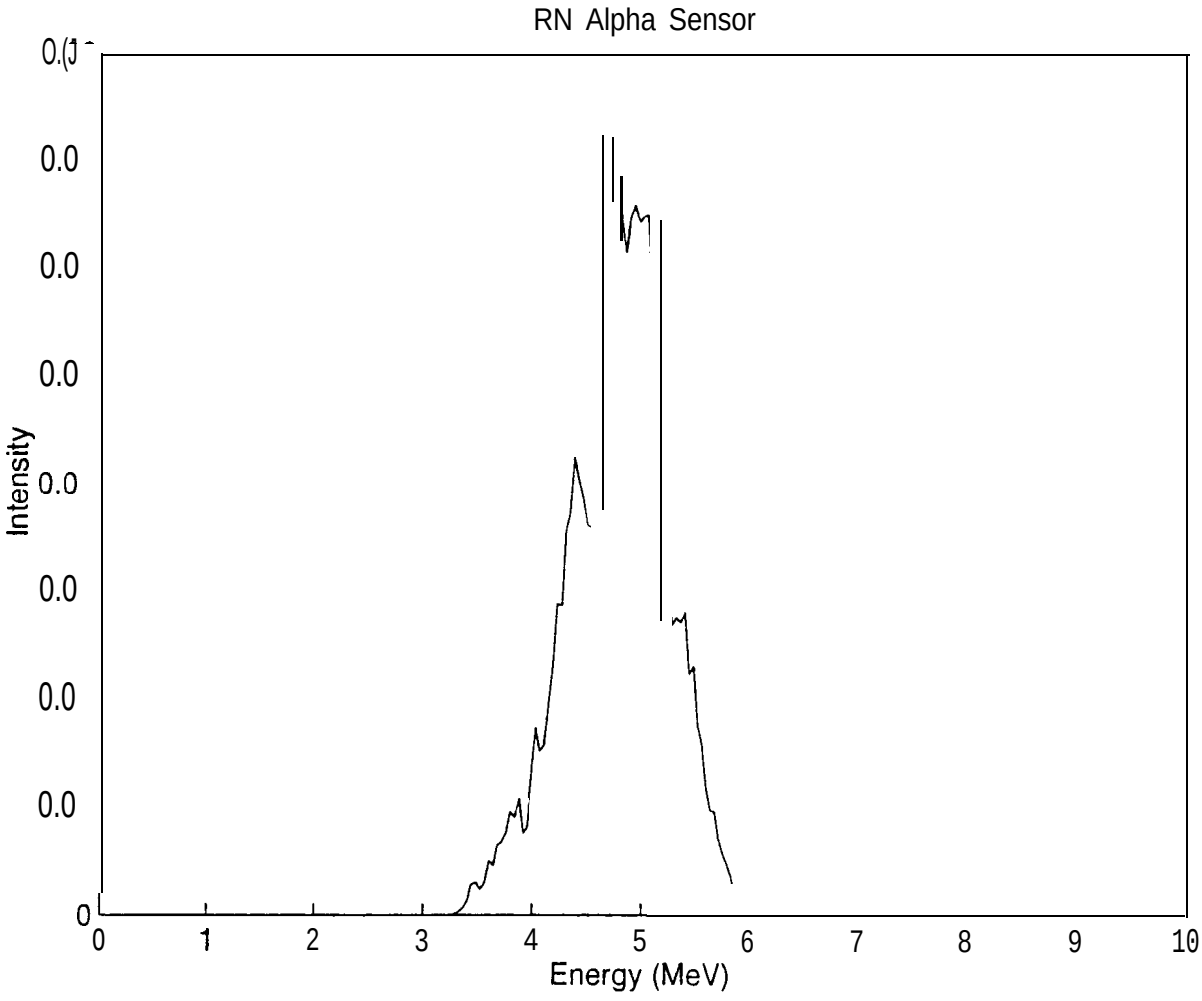


**Figure 3-11. RN A1pha Sensor Thorium-230 measured simultaneously with the HSGC-MS data**

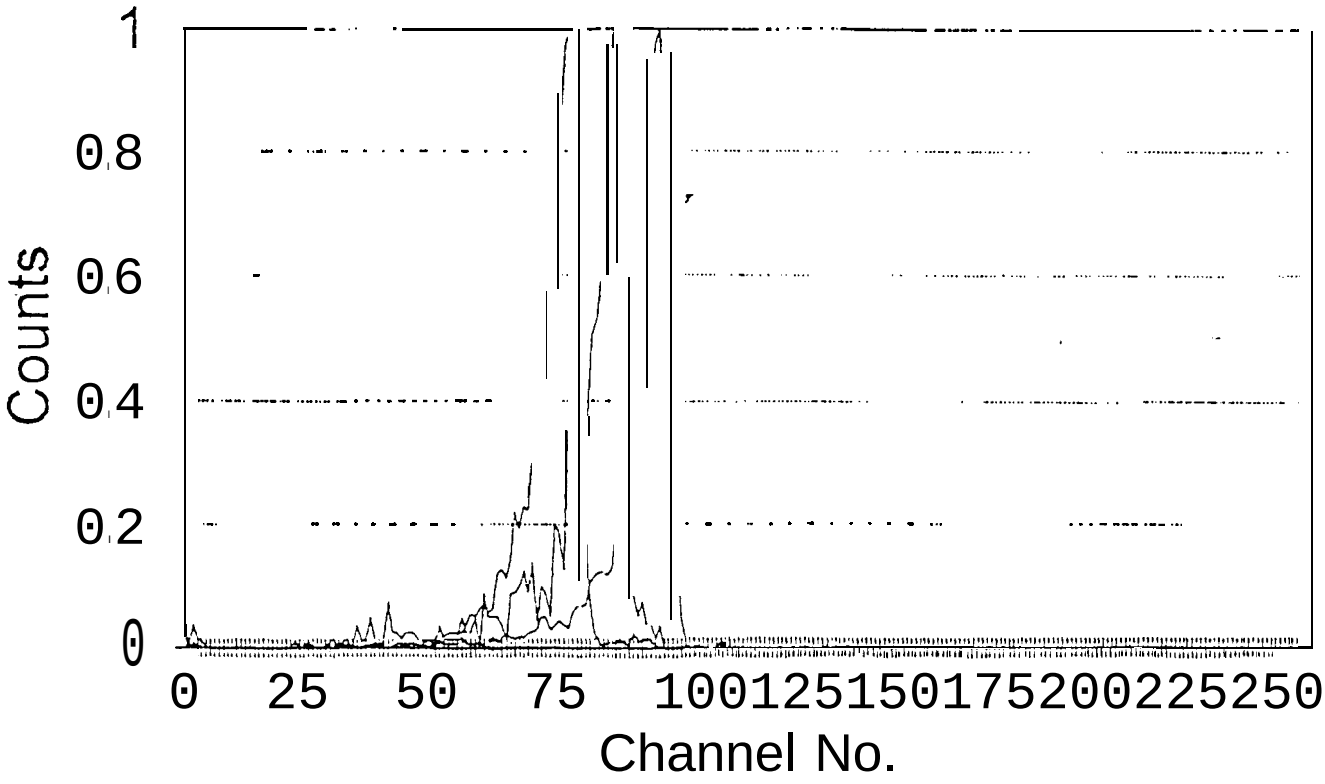


**Figure 3-12. Th, Pu, Am Discrimination**

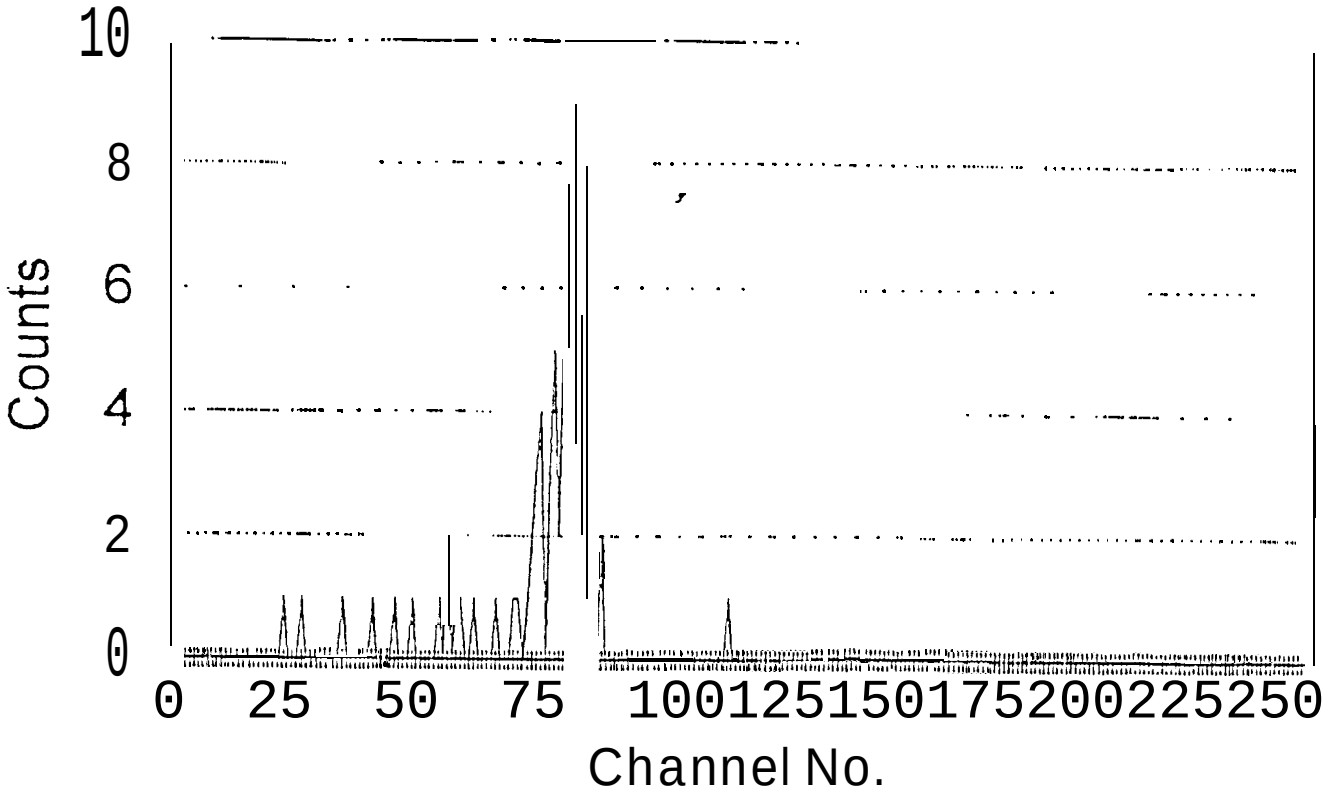


**Figure 3-13. Alpha Sensitivity Test Using Th on Concrete**

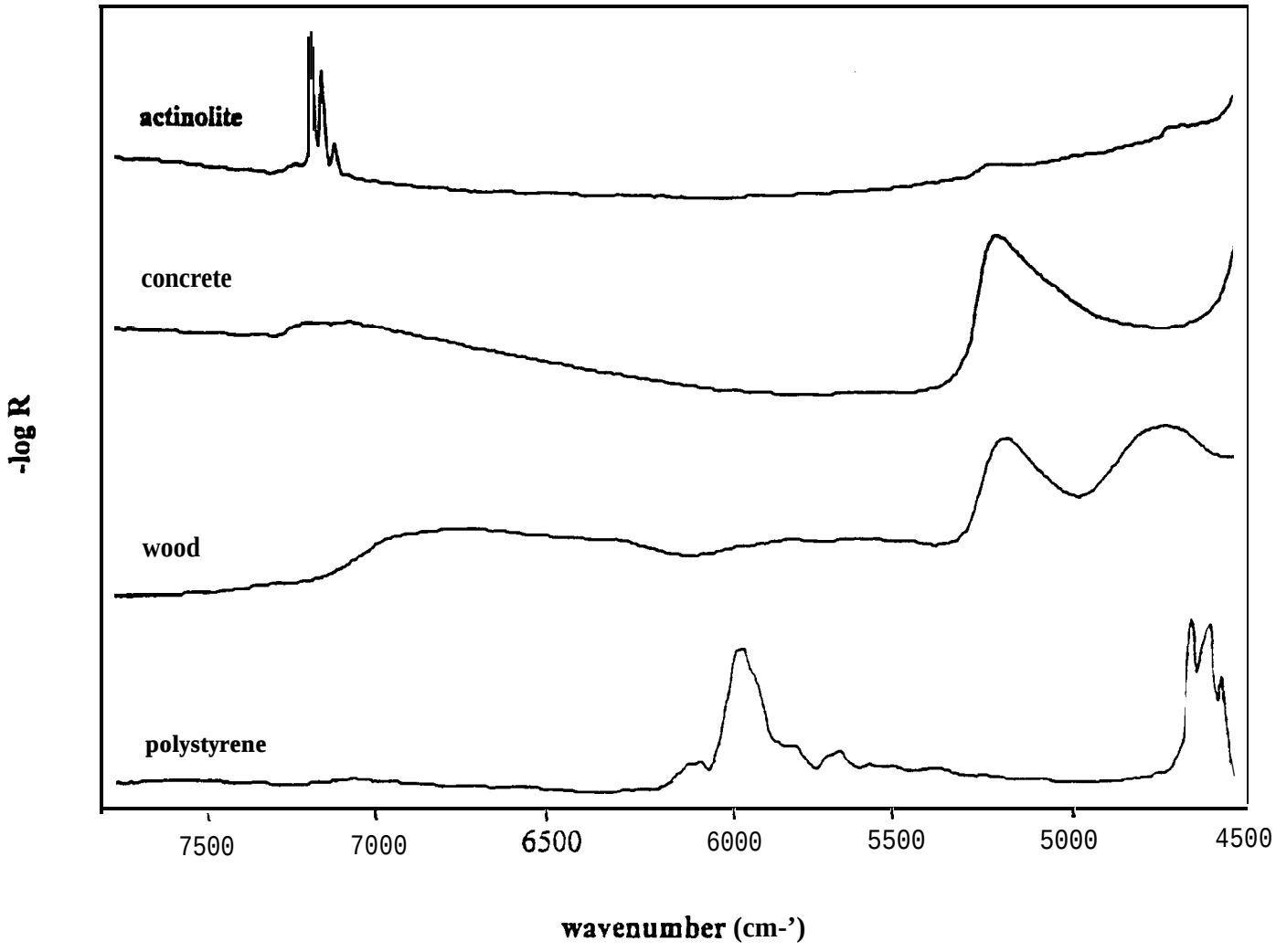


**Figure 3-14. Typical NIR Spectrum Measured in 45 Seconds using a Slica 7-around-1 Probe and Mattson Spectrometer**

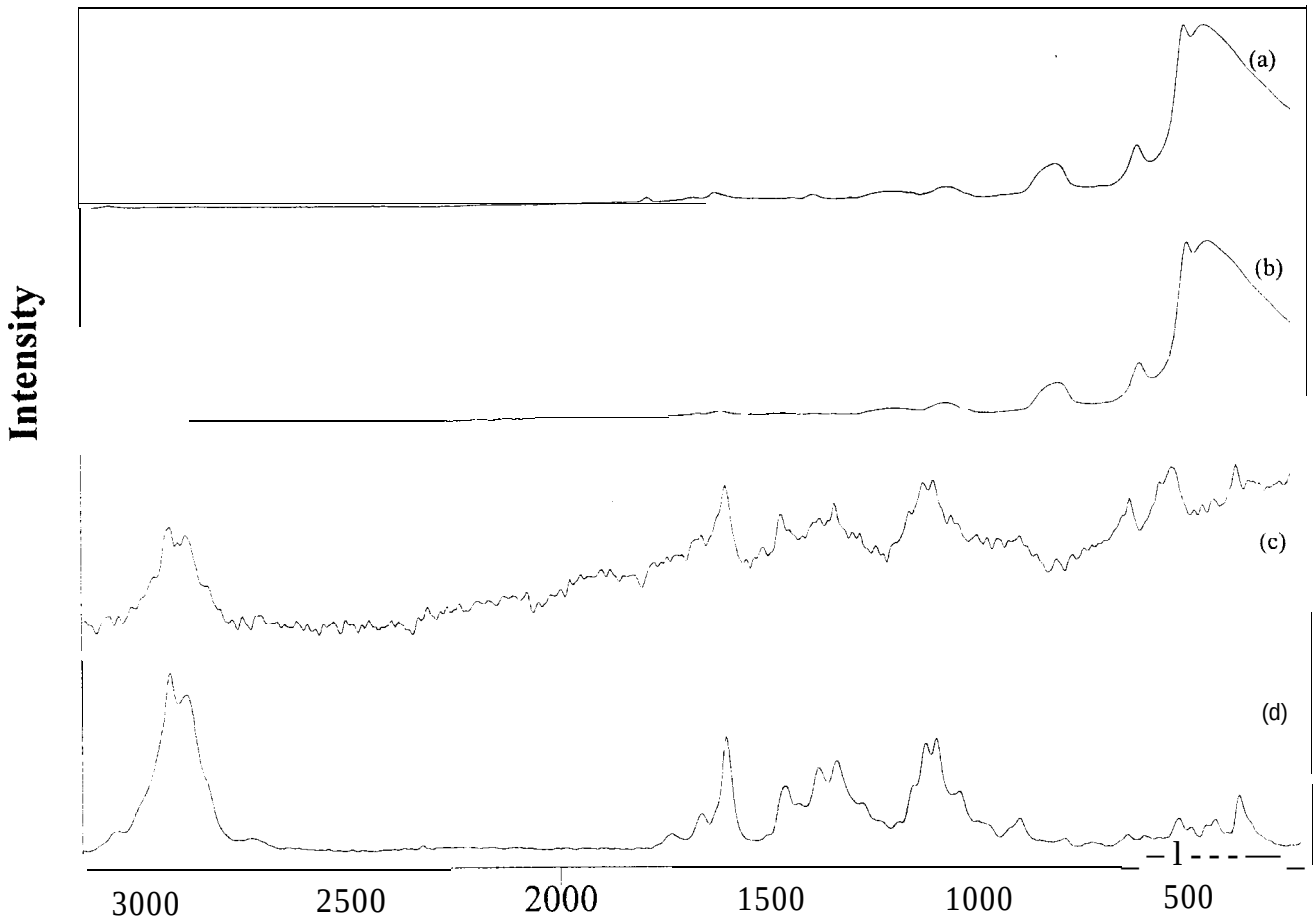


**Figure 3-15. Typical Raman spectroscopic performance of an unfiltered focused fiber-optic probe. (a) silica background, (b) balsa wood + silica background,(c) resultant spectrum calculated by scaled subtraction of b-a, and (d) spectrum of balsa wood measured in macro sample compartment.**

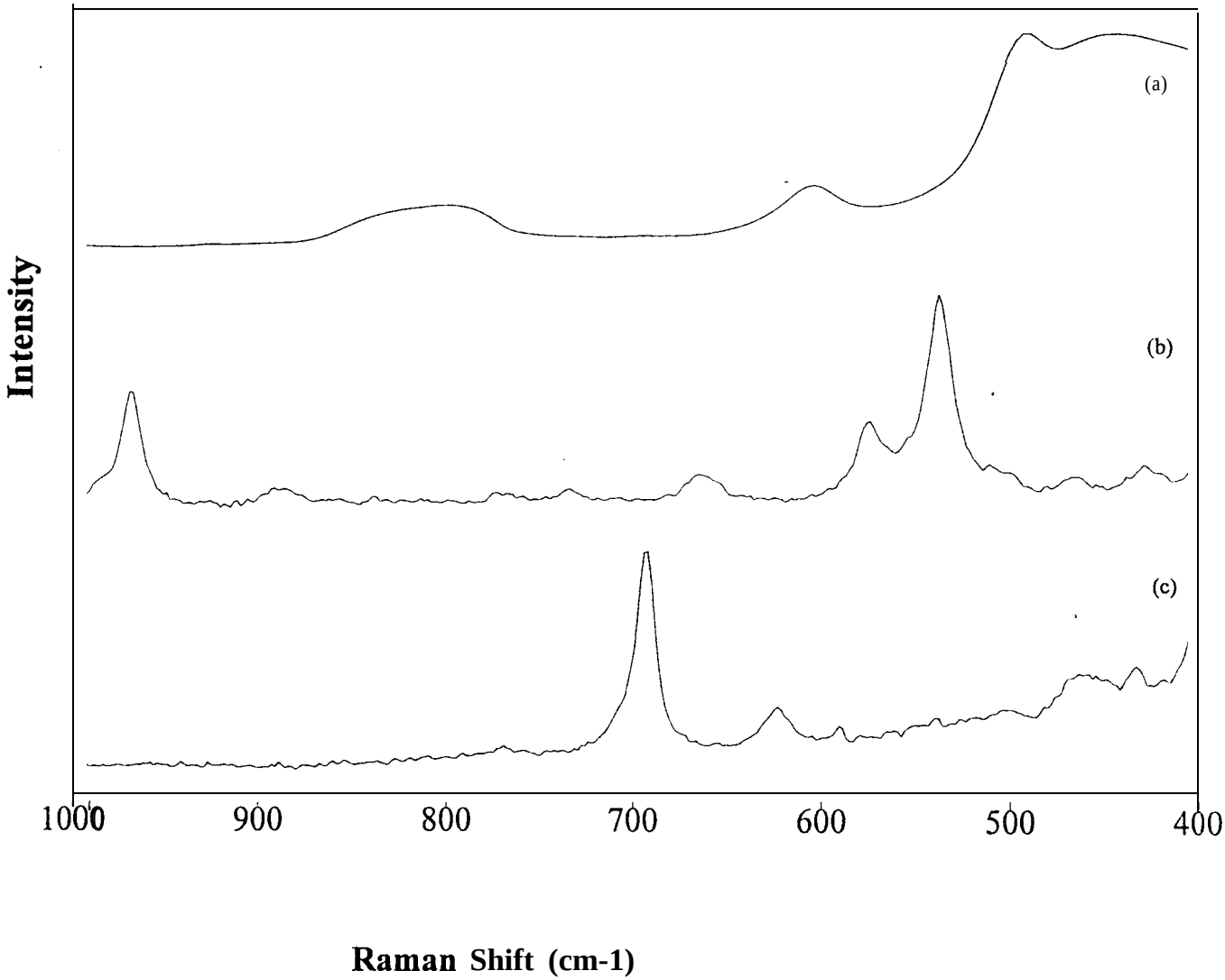


**Figure 3-16. Raman spectra in the wavenumber range 1200400 cm-' of(a) typical silica background, (b) crocidolite, and (c) chrysotile.**

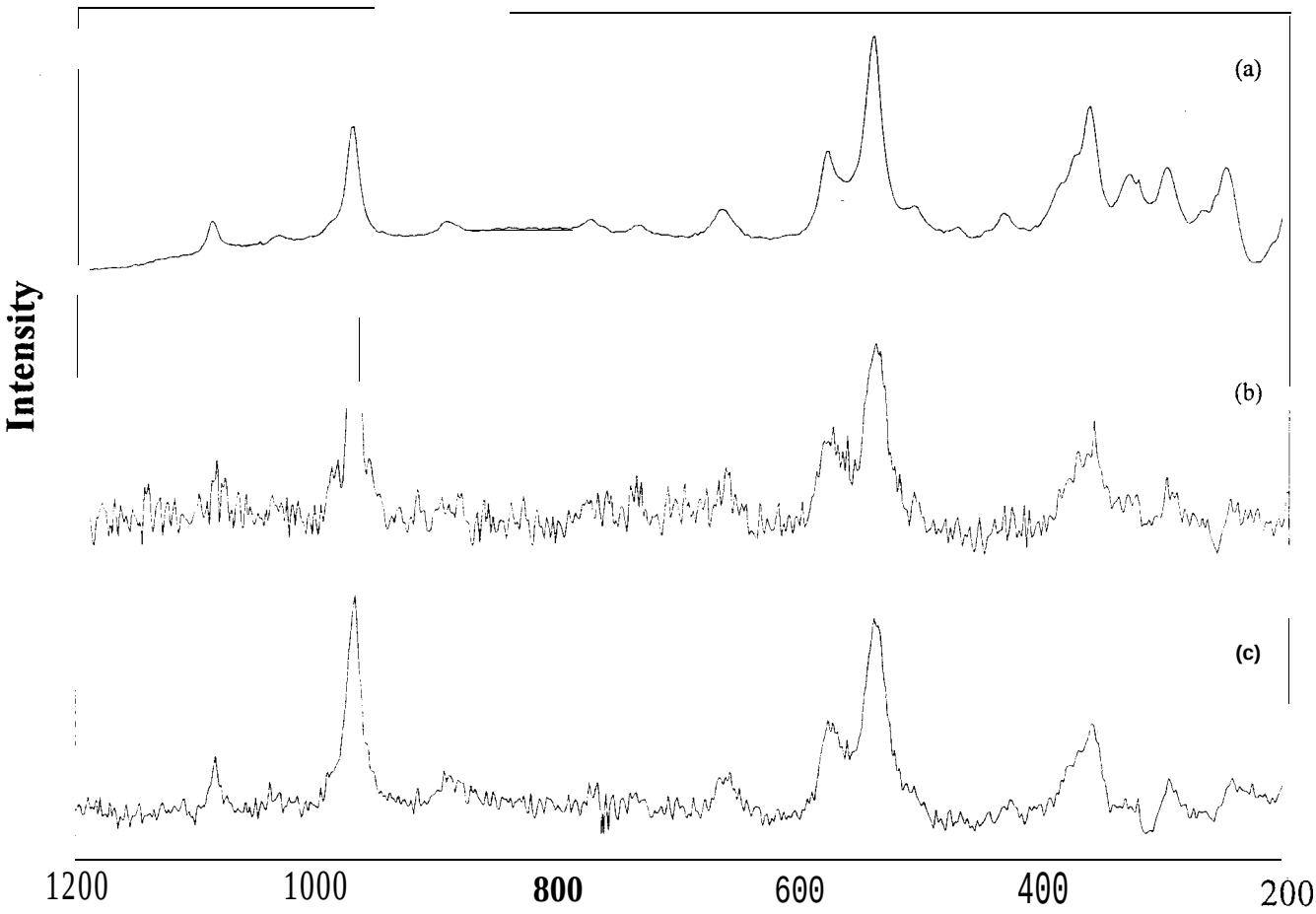


**Figure 3-17. Raman spectra of the asbestos mineral crocidolite recorded using (a) Renishaw microscope, 785 nm, 2.5 mW, 30 sec. CCD integration time, 100 coadded scans, (b) Kaiser Holoprobe, 785 nm, 5 mW, 20 sec. CCD integration time, 1 scan, and (c) Kaiser Holoprobe, 785 nm, 5 mW, 120 sec. CCD integration time, 1 scan.**

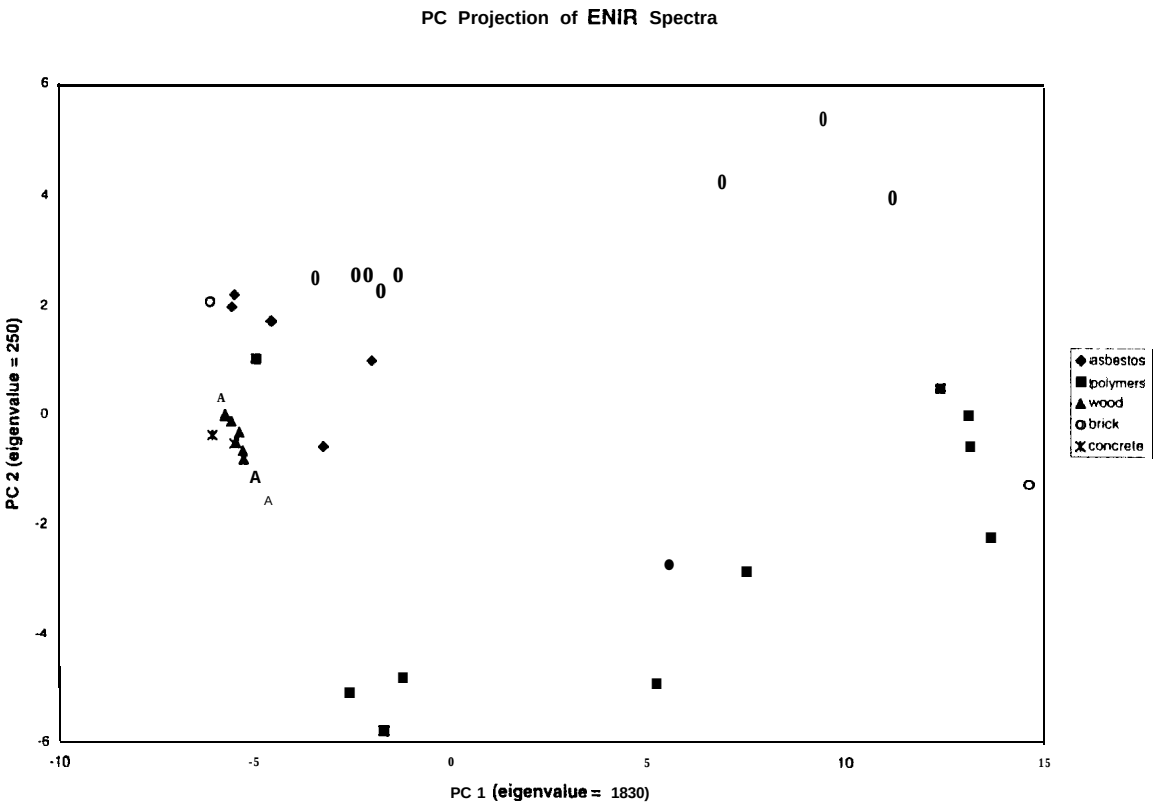


**Figure 3-18. Plot of PC1 *vs.* PC2 for the PCA of the ENIR DR spectra of several samples of asbestos (♦), polymers (■), wood (A), brick (0) and concrete (*). Although some clustering can be seen on this plot, it is not possible to define regions by which the nature of a given sample can be assigned unambiguously.**

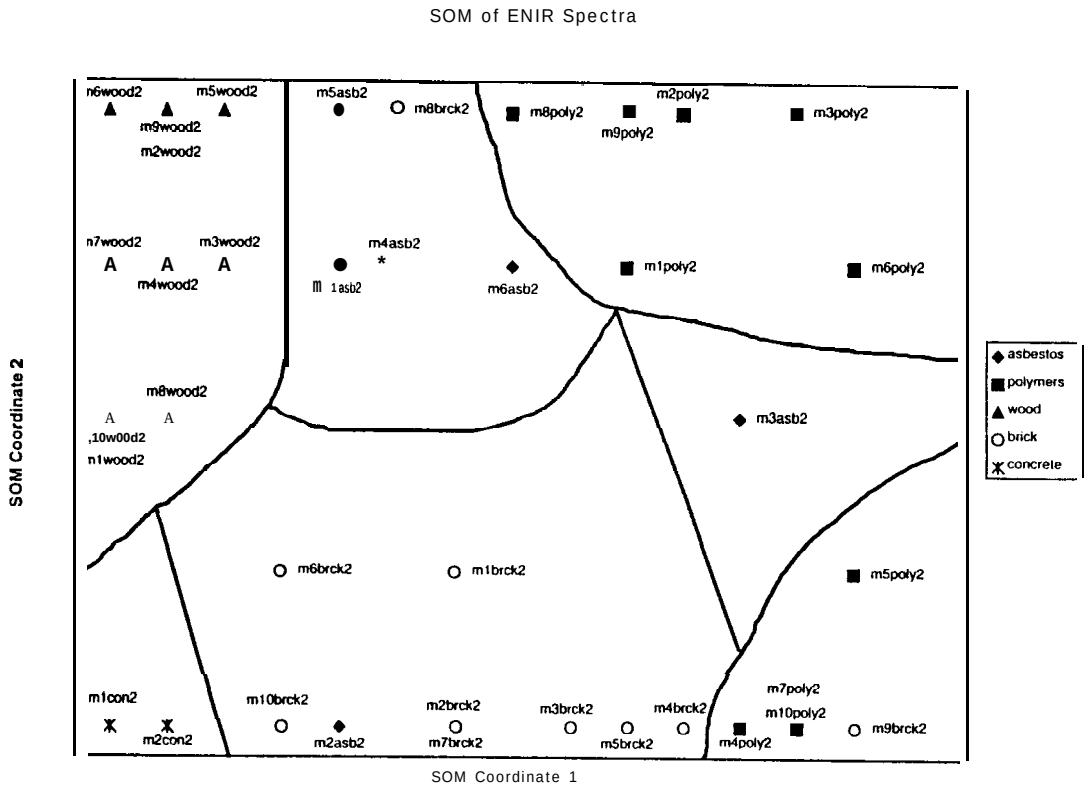


**Figure 3-19. Plot of Coordinate 1 *vs.* Coordinate 2 for a SOM calculated for the ENIR DR spectra of the same samples of asbestos (♦), polymers (■), wood (A), brick (0) and concrete (*) used in Figure 2-20. Regions appearing to bound the spectra of each type of sample are delineated with bold lines.**